

## Pairing of Composite Fermions

Bonesteel, N.E., NHMFL/FSU, Physics

The composite Fermi liquid (CFL) description of the two-dimensional electron gas at Landau level filling factor  $\nu=1/2$  in terms of a “metal” of composite fermions in zero effective magnetic field appears now to have been confirmed by a number of experiments. The mathematical formulation of this description is based on representing physical electrons by Chern-Simons (CS) fermions coupled to a CS gauge field.

Recent numerical calculations<sup>1</sup> suggest that the experimentally observed  $\nu=5/2$  fractional quantum Hall state, in which the effective filling fraction of the first excited Landau level is  $\nu=1/2$ , may be a  $p$ -wave “superconductor” of composite fermions described by the Pfaffian wave function introduced by Moore and Read. It is, therefore, natural to ask what effect the CS gauge field may have on BCS pairing.

In order to address this question the simplest possible model containing the essential physics of this system has been studied.<sup>2</sup> This model describes a two-dimensional gas of spin-1/2 fermions coupled to a CS gauge field and interacting via an attractive  $s$ -wave interaction. In the absence of the CS gauge field the model is, of course, unstable to a paired state for arbitrarily weak pairing interaction. When fluctuations of the CS gauge field are included the pairing transition is driven first order and the CS Fermi sea is *stable* for weak enough pairing interactions. Such a first-order pairing transition is illustrated in Figure 1, which shows the  $T=0$  condensation energy of a CFL as a function of the BCS coupling constant  $\lambda$ . For small enough  $\lambda$  there is no transition and the

CFL is stable, but as  $\lambda$  increases a first-order transition eventually occurs.

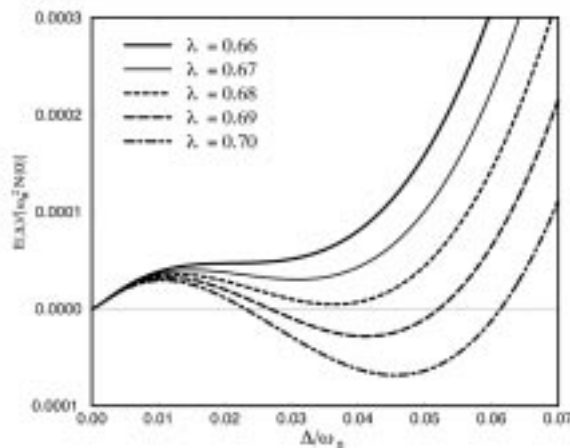


**Figure 1.** Condensation energy vs. gap parameter for different values of the BCS coupling constant  $\lambda$  in a composite Fermi liquid. A first-order phase transition with a discontinuous jump in  $\Delta$  is seen to occur as  $\lambda$  increases.

In addition to this simplified model, the more physically relevant case of  $p$ -wave pairing of spin-polarized CS fermions interacting via the Coulomb repulsion has also been studied, with similar results.<sup>3</sup> At this time, the main conclusions of this work are (1) the pair-breaking effects of the CS gauge field may be the reason that the  $\nu=1/2$  CFL state does *not* undergo a pairing instability; and (2) any pairing transition of the CFL (for example, one driven by tilting the magnetic field) is predicted to be *first order*.

### References:

- <sup>1</sup> Park, K., *et al.*, Phys. Rev. B, **58**, 10167 (1998).
- <sup>2</sup> Bonesteel, N.E., preprint.
- <sup>3</sup> Bonesteel, N.E., Phys. Rev. Lett., in press. (cond-mat/9807146).

## 2-D Spin Distributions and Magnetization Steps in Single ZnSe/Zn(Cd, Mn)Se Quantum Wells

Crooker, S.A., NHMFL/LANL

Rickel, D.R., NHMFL/LANL

Kikkawa, J.M., Univ. of California-Santa Barbara,  
Physics

Awschalom, D.D., Univ. of California-Santa  
Barbara, Physics

Smorchkova, I.P., Pennsylvania State Univ., Physics

Samarth, N., Pennsylvania State Univ., Physics

Using the recently developed capability for performing high-speed optical spectroscopy in the 60 T Long-Pulse magnet at the NHMFL-Los Alamos, we performed low temperature photoluminescence (PL) measurements of single ZnSe/Zn(Cd, Mn)Se quantum wells to 60 T. These MBE-grown 12 nm wide single quantum well samples contain local magnetic spins ( $\text{Mn}^{2+}$ ) incorporated in “digital” fashion; that is, in discrete monolayer (ml) and fractional-monolayer planes of the magnetic semiconductor MnSe. In this way, even though each sample contains the same number of embedded  $\text{Mn}^{2+}$  moments, the *local* magnetic environment can be tuned independently from electronic interactions. Thus, the statistics of  $\text{Mn}^{2+}$  spin clustering in these structures can be directly controlled—the relative percentages of isolated  $\text{Mn}^{2+}$  spins vs. pairs of nearest-neighbor  $\text{Mn}^{2+}$  spins, vs. higher-order spin clusters can be varied through the amount of fractional-monolayer MnSe coverage.

Low temperature (350 mK) PL from these samples reveals a giant Zeeman shift of the fundamental heavy-hole exciton resonance owing to the large *sp-d* exchange interaction between charge carriers (electrons and holes) and the *d*-electrons that comprise the local  $S=5/2$   $\text{Mn}^{2+}$  moment. The exchange interaction dominates all other energy scales in this problem,

and thus the Zeeman shift is directly proportional to sample magnetization. Photoluminescence from three structures containing (respectively) 1/4 ml, 1/2 ml, and full-monolayer planes of MnSe are shown in Figure 1. The data reveals a clear saturation of the isolated paramagnetic spins by 10 T in all samples, followed by a high-field, sample-dependent susceptibility that is a consequence of spin clustering. When the *local* magnetic density is low (e.g., for the sample with 1/4 ml MnSe planes), there is a preponderance of Mn-Mn nearest neighbor pairs; these antiferromagnetically-bound pairs exhibit a staircase-like susceptibility as the magnetic field drives their total spin from  $S=0$  to  $S=1, 2, \dots, 5$  at multiples of the nearest-neighbor exchange field  $J_{\text{NN}}$ . By comparison, a much more linear high-field susceptibility is obtained in samples with large local Mn density (e.g., full monolayers of MnSe) where the majority of Mn spins are bound up in large clusters with long-range antiferromagnetic correlations.

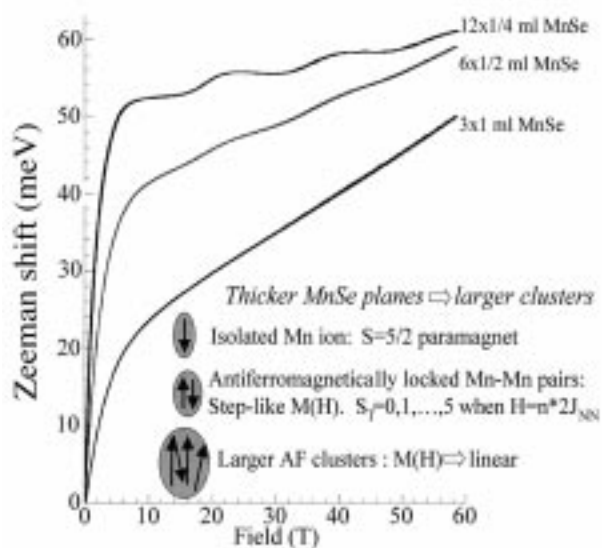


**Figure 1.** Measured Zeeman shift from magnetic quantum wells containing 1/4 ml, 1/2 ml, and full-monolayer planes of MnSe. High-field susceptibilities reflect the different local magnetic densities and Mn spin-clusters.

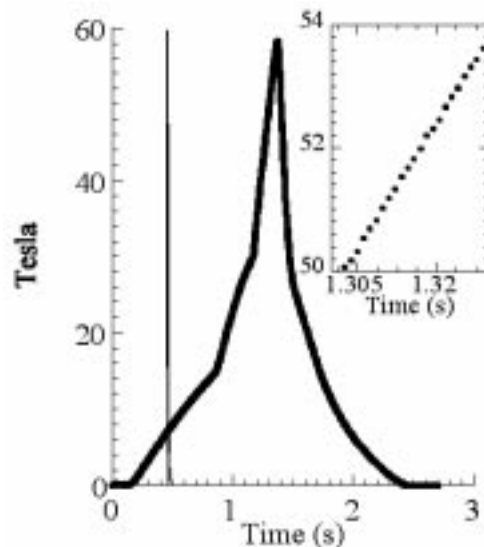
## High-Speed Optical Spectroscopy in the 60 Tesla Long Pulse Magnet

Crooker, S.A., NHMFL/LANL  
Rickel, D.G., NHMFL/LANL

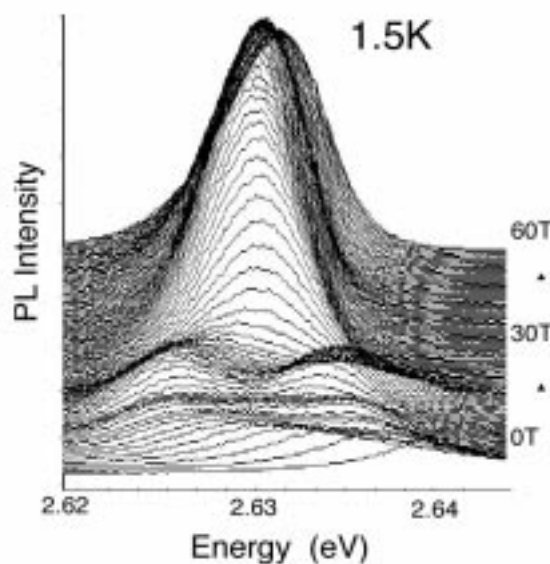
The extremely long two-second duration of the 60 T Long Pulse (LP) magnet at the NHMFL-Los Alamos represents an increase of over two orders-of-magnitude of time “at-field” as compared with traditional capacitor-driven pulsed magnets. This increase has tremendous implications for high-resolution optical spectroscopy in pulsed magnetic fields—in particular, in conjunction with modern CCD detectors it is now for the first time possible to perform *continuous* high-speed (kHz-rate) acquisition of optical spectra throughout an entire 60 T magnet pulse with very little field variation between spectra. Typically, over 2000 complete spectra are obtained during a 60 T LP magnet shot, allowing complete (and timely) reconstruction of an entire spectra-vs.-field dependence in a variety of condensed matter systems. Experiments to date have focused on photoluminescence studies of both magnetic and nonmagnetic semiconductor quantum structures.

Figure 1 shows the typical field profile of the 60 T LP magnet used for optics experiments (a 60 T capacitor-driven “short pulse” magnet profile is also shown for comparison). For optics experiments it is advantageous to stretch out the upsweep of the magnet as long as possible so as to achieve the smallest possible dB/dt. The inset shows an expanded portion of the steepest part of the field ramp, where each point represents the acquisition of a complete optical spectra. With  $\sim 1.2$  ms exposure time, the field variation is only 165 mT between spectra, so that small features in the optical spectra can now be recovered with a high degree of precision and confidence. For example, Figure 2 shows a subset of photoluminescence data taken from a magnetic 2-D electron gas acquired during a

single upsweep of the 60 T LP magnet, where clear intensity and wavelength oscillations are observed as the Fermi level moves through integer quantum Hall levels.



**Figure 1.** Field profile of the 60 T Long Pulse magnet, with a capacitor-driven magnet field profile shown for comparison. Inset: An expanded view, showing actual points at which spectra were acquired.



**Figure 2.** A sample of the raw data taken on the upsweep of the 60 T Long Pulse magnet. Over 2000 spectra are typically acquired in a single magnet shot.

The optical system we employ is designed with an aim toward maximum coupling and detection efficiency from 250 nm to 900 nm. These considerations are of paramount importance when, for instance, collecting photoluminescence spectra from weakly-emitting samples on millisecond

timescales. Laser excitation and collected signal are coupled to and from the sample through single 200- or 600-micron diameter glass optical fibers. The sample is in direct contact with the other end of the fiber. Fibers are chosen to have low numerical apertures (NA~0.16) so as to best couple the light to an optically fast (f/4) 300 mm focal length spectrometer (Acton 308). The multichannel detector is a commercial liquid-nitrogen cooled, backthinned CCD (Princeton Instruments) with 1340x100 pixels that is designed for extremely high quantum efficiency and fast readout. The quantum efficiency of this device is ~90% at 600 nm and ~45% at 350 nm, and its low-noise digitizer operates at 1 MHz with 14-bit resolution. The full array can be continuously binned, digitized, and streamed to computer in 2.1 ms (476 Hz) over a high-speed PCI data bus. Hardware chip redefinitions and modified binning result in acquisition rates up to 1 kHz. The sensitivity of the CCD, efficient optical coupling, and the comparatively long millisecond exposure times allow excellent signal:noise even in a PL experiment with low laser excitation intensity (~100 microwatts in Figure 2).

These optics experiments are now also being performed at Los Alamos in the capacitor-driven 42 T pulsed magnet, designed by L. Li and B. Lesch (NHMFL-Tallahassee), which has a 500 ms pulse duration.

## Optical Signatures from Magnetic 2-D Electron Gases at High Fields to 60 Tesla

Crooker, S.A., NHMFL/LANL

Rickel, D.R., NHMFL/LANL

Kikkawa, J.M., Univ. of California-Santa Barbara, Physics

Awschalom, D.D., Univ. of California-Santa Barbara,

Physics

Smorchkova, I.P., Pennsylvania State Univ., Physics

Samarth, N., Pennsylvania State Univ., Physics

Recent advances in II-VI molecular-beam epitaxy now permit the growth of two-dimensional electron gases (2DEGs) in *magnetic* semiconductor quantum

structures. Unlike their nonmagnetic III-V semiconductor counterparts, these new 2DEGs can be incorporated directly into quantum wells containing local magnetic moments (typically  $\text{Mn}^{2+}$  ions), allowing for the intriguing possibility of studying the physics of a mobile gas of electrons whose spins are strongly exchange-coupled to a matrix of embedded magnetic moments.

High field photoluminescence (PL) studies of magnetic 2DEG systems have been performed at the NHMFL-Los Alamos in the 60 T Long Pulse magnet. In this field regime, the local Mn moments are driven into nearly complete saturation. The samples are modulation-doped ZnSe/Zn (CdMn) Se single quantum wells with carrier densities  $n_c \sim 5 \times 10^{11}$  electrons/cm<sup>2</sup>. Owing to the strong  $J_{sp-d}$  exchange interaction in these II-VI systems, the Zeeman energies (spin-splittings) in the conduction band are comparable to or even larger than the cyclotron energies (Landau-level splittings), so that the 2DEG is highly spin-polarized even at low magnetic fields.

PL data reveal a highly anomalous Zeeman shift of the fundamental PL peak with increasing field. As shown in Figure 1, the energy shift of the PL no longer resembles the Brillouin-function-like Zeeman shift that would be expected of paramagnetic  $\text{Mn}^{2+}$

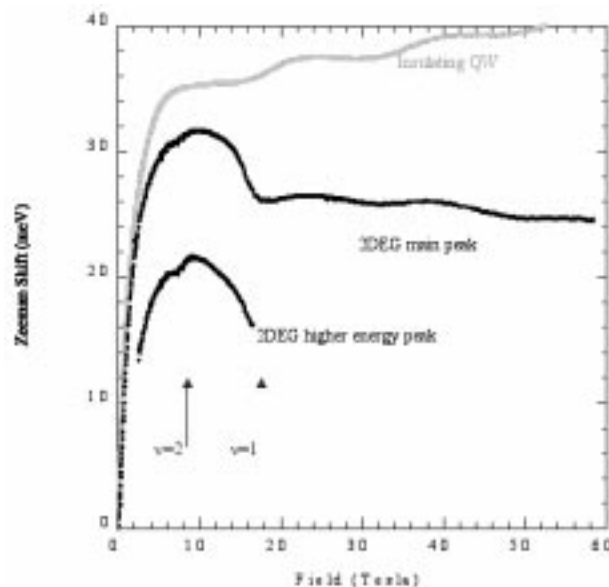


**Figure 1.** Measured Zeeman shift of the PL peaks from a magnetic 2DEG at 350 mK. Data from an insulating magnetic QW shown for comparison.

moments. Rather, there exists a pronounced maximum in the Zeeman shift near  $\nu=2$  and a clear kink at quantum Hall filling factor  $\nu=1$ . In this field regime there also exists a higher-energy satellite peak that appears at low fields, grows in intensity, and finally disappears at  $\nu=1$  (its energetic shift is also plotted). The higher energy satellite peak tracks the fundamental PL peak with a constant separation of  $\sim 10$  meV, and is thus not a higher-lying Landau level. This behavior is observed in many different magnetic 2DEG samples with different magnetic environments and carrier densities, and ongoing experiments are aimed at elucidating its origin.

Figure 2 shows an example of the clear oscillations in the integrated PL intensity observed in magnetic 2DEG samples. This behavior is a common feature of semiconductor electron gases and corresponds to the Fermi level moving through integer Landau levels. In contrast with nonmagnetic 2DEGs, however, these oscillations correspond to every-integer (rather than even-integer) filling factors arising from the highly spin-polarized nature of the magnetic 2DEG.

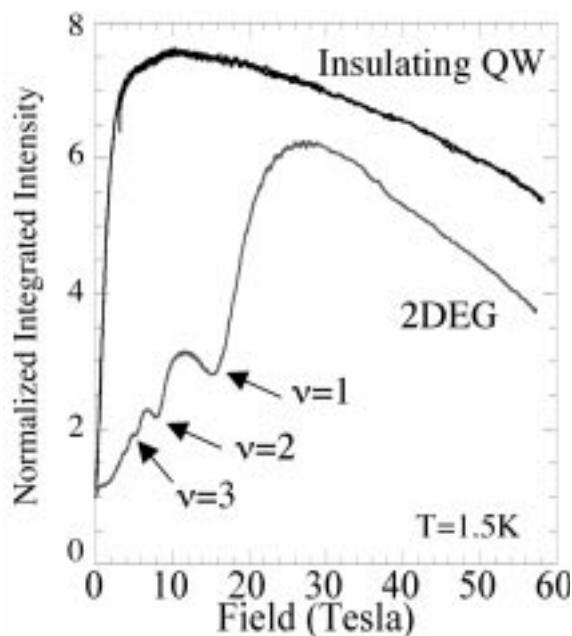


**Figure 2.** Integrated intensity from a magnetic 2DEG, showing every-integer filling factors. Data from an insulating magnetic QW shown for comparison.

## Physics of Deep Levels in Semiconductor Quantum Dots

Dow, J., Arizona State Univ., Physics

Semiconductor quantum dots offer promise for providing enhanced catalysis, as well as optical semiconductors, whose band gaps have frequencies further into the blue and ultraviolet portions of the spectrum than conventional devices. The deep impurity levels in such quantum dots, however, are currently not well understood, although they are known experimentally to often trap carriers, and to facilitate catalytic processes.

To elucidate the physics of deep levels in semiconductor quantum dots, we have developed a theory that shows that the deep levels themselves are relatively insensitive to quantum confinement as the dot-size shrinks, but that the band edges move away from the center of the gap as the dot-size contracts. Since it is the interplay between the impurity deep level energies, and the intrinsic band-edge energies that determines whether an impurity is, for example, a shallow donor, a deep trap, or even a shallow acceptor, we have made a series of predictions of such interplay for chalcogen impurities in Si to illustrate how the dot-size influences the behavior of the electronic states. These predictions are meant to stimulate electron-spin resonance measurements that will be used to test the theory, and to quantitatively demonstrate the host-like and antibonding character of the deep levels, which can be exploited to tailor the electronic and optical properties of doped quantum dots.

*Reference:*

- 1 Song, J., *et al.*, Phys. Rev. B, in press.

# Mesoscopic Fluctuations of Chiral Surface Sheaths in the Integer Quantum Hall Effect

Druist, D.P., Univ. of California at Santa Barbara, Physics

Gwinn, E.G., Univ. of California at Santa Barbara, Physics

Yoo, K.-w., Korea Institute of Standards and Science

Maranowski, K., Univ. of California at Santa Barbara, Electrical and Computer Engineering

Gossard, A.C., Univ. of California at Santa Barbara, Electrical and Computer Engineering

We have demonstrated recently the existence of a new class of 2D system, the chiral surface sheath that forms from coupled edge states at the boundaries of semiconductor multilayers in the quantum Hall regime.<sup>1</sup> The uni-directional flow around the perimeter of this "chiral" metal give it unusual transport properties, by suppressing the localization characteristic of ordinary low-dimensional systems.<sup>2</sup> We are using this new system to probe dephasing by electron-electron scattering, the dominant mechanism for loss of coherence at the temperatures of interest.

Measurements made at NHMFL focussed on a new set of GaAs/AlGaAs multilayer samples with ~2 meV bandwidth, much larger than we had studied previously. Only the  $\nu = 2$  per layer quantum Hall state was well-developed at low temperatures (in contrast to lower density, narrow-bandwidth multilayers, which had quantum Hall states at  $\nu = 1, 2$  and 4 per layer). Vertical transport data on a set of multilayer pillars with diameters from 100  $\mu\text{m}$  to 4  $\mu\text{m}$  showed wider quantum Hall states in smaller samples. These samples were dry-etched to have vertical sidewalls, and mounted at a small angle relative to the field. The amplitude of the reproducible fluctuations in the vertical conductance suggest that the phase coherence length on the surface sheath is ~10  $\mu\text{m}$ .<sup>3</sup>

## References:

- 1 Druist, D.P., *et al.*, Phys. Rev. Lett., **80**, 365 (1998).
- 2 Balents, L., *et al.*, Phys. Rev. Lett., **76**, 2782 (1996).
- 3 Druist, D.P., *et al.*, "Conductance Fluctuations of Chiral Metals," to appear in Superlattices and Microstructures.

# Magnetotransport in AlGaAs/GaAs Multiple Quantum Wells

Du, R.R., Univ. of Utah, Physics

Zudov, M.A., Univ. of Utah, Physics

Simmons, J.A., Sandia National Laboratories

Reno, J.L., Sandia National Laboratories

In a study of electrodynamic response of the quantum Hall system, we employ AlGaAs/GaAs multiple quantum wells (QW) for microwave transmission measurements. High quality AlGaAs/GaAs structures were grown by MBE at Sandia National Laboratories. Figure 1 shows data of magnetoresistance,  $R_{xx}$ , and Hall resistance  $R_{xy}$  in one sample having electron density in each well  $n_s = 1.1 \times 10^{11}/\text{cm}^2$  and mobility  $\mu = 1 \times 10^6 \text{ cm}^2/\text{Vs}$ . The sample has 40 identical, 30 nm wide GaAs wells, confined by  $\text{Al}_{0.1}\text{Ga}_{0.9}\text{As}$  barriers; the separation of wells is 270 nm.

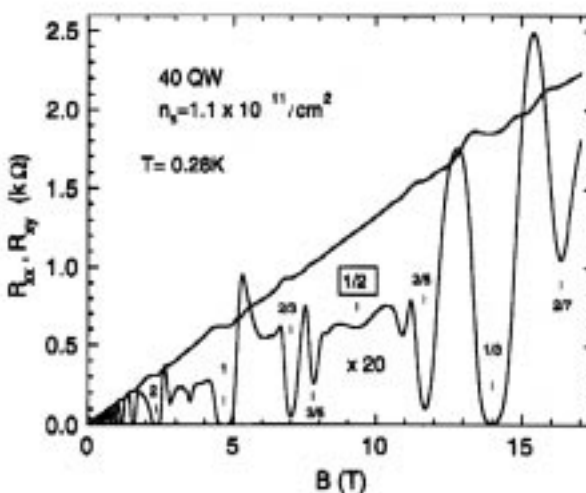


Figure 1. The magnetoresistance  $R_{xx}$ , and Hall resistance  $R_{xy}$ , measured in a 40-AlGaAs/GaAs quantum well sample at temperature  $T = 0.28 \text{ K}$ .

The sample measured is a standard Hall bar. AuGeNi contacts were diffused on the side edge of the mesa, which allowed successful connections to all 40 electron layers in the sample.

Our data show high quality of the two-dimensional (2D) electron gas in the QWs. Around the Landau level filling factor  $\nu=1/2$  the fractional quantum Hall states at  $\nu=1/3$ ,  $2/5$ ,  $3/7$ , and at  $\nu=2/3$ ,  $3/5$  are clearly resolved at temperature  $T = 0.28$  K. These data are comparable with that measured in an electron system in AlGaAs/GaAs heterostructure with similar density and mobility. Sharp  $R_{xx}$  minima observed from the sample support the notion that the electron densities are remarkably uniform among different layers. The  $R_{xy}$  structures near the quantum Hall plateaus indicate, however, some discrepancies of electron densities which could result from the top and bottom layers of the sample.

Further experiments of magnetotransport at still higher magnetic field using this type of sample would be very interesting. In this situation, the thickness of the 2D electron well exceeds the magnetic length, therefore the electron-electron interaction may be modified from the pure Coulomb interaction.

This work is supported by NSF grant DMR-9705521. Sandia is supported by DOE under contract DE-AC05-94AL85000.

#### Reference:

*Perspectives in Quantum Hall Effect—Novel Quantum Liquids in Low-Dimensional Semiconductor Structures*, ed. by S. Das Sarma and A. Pinczuk, Wiley and Sons, New York, 1997.

## Suppression of the Two-Dimensional Metallic Phase by Spin-Flip Scattering

Feng, X.G., NHMFL

Popovic, D., NHMFL

Washburn, S., Univ. of North Carolina-Chapel Hill, Physics

The existence of a metallic state and a metal-insulator transition (MIT) has been established recently in a variety of two-dimensional electron and hole systems (2DES and 2DHS) with a sufficiently high mobility. On the other hand, low mobility samples are known to display only insulating behavior. Clearly, the disorder plays an important role, but a transition between a 2D metal and an insulator as a function of *disorder* has not been investigated experimentally in detail until now. We have studied this problem by carrying out detailed measurements of the temperature ( $T$ ) dependence of conductivity ( $\sigma$ ), for  $0.3 < T < 4.5$  K, over a wide range of carrier densities ( $n_s$ ), up to  $10^{12}$  cm<sup>-2</sup>, for different values of disorder.

The experiment was performed on a 2DES in Si metal-oxide-semiconductor field-effect transistors, and the disorder was varied using substrate (back-gate) bias  $V_{sub}$ . For each given  $n_s$ , the disorder was characterized by the (inverse) Drude (4.2 K) mobility. The reverse (negative)  $V_{sub}$  moves the electrons closer to the interface, which *increases* the oxide charge scattering and scattering due to the roughness of the Si-SiO<sub>2</sub> interface, but it *decreases* the scattering by electrons from long band tails in upper subbands as it increases the subband splitting. As a result of these competing effects, we find that the disorder at the lowest and highest  $n_s$  increases, whereas the disorder in the intermediate range of  $n_s$  decreases with increasing (negative)  $V_{sub}$ , as expected. The metallic behavior (increase of  $\sigma$  as  $T$  is lowered) emerges in this intermediate range of  $n_s$ . In particular, for a given  $n_s$ , the metallic behavior spreads out toward lower  $T$  with the increasing reverse  $V_{sub}$ . At the lowest  $T$ , however,

the temperature dependence of  $\sigma$  is insulating. In other words,  $\sigma(T)$  displays a *maximum*, with the position of the maximum  $T_m$  shifting to lower  $T$  with increasing reverse  $V_{sub}$ , i. e. as the scattering by electrons localized in the tail of the upper subband is reduced. For sufficiently large  $V_{sub}$ , i. e. for sufficiently large subband splitting, the upper subband is completely depopulated. Indeed, we find that  $T_m$  extrapolates to zero when the subband splitting becomes of the order of 30 meV, and  $\sigma(T)$  then becomes metallic for all  $n_s > n_c$  ( $n_c$  - critical density). The properties of the 2D MIT under those conditions are the same as those observed in other 2D systems. Further increase in (reverse)  $V_{sub}$  leads only to a considerable increase of the disorder at all  $n_s$  but without a significant effect on  $\sigma(T)$ .

Clearly, the scattering by electrons localized in the upper subband has a much more detrimental effect on the metallic behavior than the other two scattering mechanisms (oxide charge and surface roughness). Since the strongly localized states deep in the band tail of the upper subband are likely to be singly populated due to a strong on-site Coulomb repulsion, they act as local magnetic moments and introduce spin-flip scattering. We have also observed adiabatic demagnetization for low values of  $V_{sub}$ . The effect vanishes for large  $V_{sub}$  when the upper subband is depopulated. This lends further support for the existence of these disorder-induced local moments in our samples. Our experiment thus suggests that in the  $T \rightarrow 0$  limit, the metallic behavior is suppressed by an arbitrarily small amount of spin-flip scattering.

## Magneto-PL Associated with a 2D Electron Gas Populating the X-Valleys in GaAs/AlAs Quantum Wells

Haetty, J., State Univ. of New York (SUNY)-Buffalo, Physics

Kioseoglou, G., SUNY-Buffalo, Physics

Petrou, A., SUNY-Buffalo, Physics

Dutta, M., ARO, Research Triangle Park

Pamulapati, J., Army Research Laboratory (ARL), Adelphi

Taysing-Lara, M., ARL, Adelphi

We have carried out a magnetoluminescence study of two GaAs/AlAs quantum wells. Sample 1 (well width 6 nm) is type-I with the lowest  $\Gamma$ -symmetry  $e_1$  subband below the AlAs X-valley. Sample 2 (well width 5 nm) is type-II with the lowest  $e_1$  subband above the AlAs X-valleys. In both samples each AlAs/GaAs/AlAs quantum well structure is flanked on either side by an n-type AlGaAs layer. The role of the AlGaAs layer is to provide electrons. In Sample 1 the resulting 2D electron gas populates the  $\Gamma$ -symmetry  $e_1$  subband and is confined in the GaAs layers. In Sample 2 the electrons populate the AlAs X-valleys instead. Thus interband transitions in Sample 1(2) are type-I, (type-II), i.e. spatially direct (indirect) in both real and k-space.

The PL from both samples is characteristic of n-type modulation doped structures, i.e. it is broad and featureless. When a magnetic field is applied distinct features appear that are attributed to interband transitions between conduction and valence band Landau levels. In Figure 1, the energies of these transitions are plotted as function of applied magnetic field. In Figure 1(b) we show the data from the type-I structure. The slopes of the interband transitions yield an electron effective mass of 0.068, which indicates that the electrons occupy the  $e_1$  subband in the GaAs wells. In Figure 1(a) we plot the data from the type-II sample. The electron effective mass determined from the slopes is 0.44, which agrees with the effective mass of the



AlAs  $X_z$ -Valleys.<sup>1</sup> Thus we conclude that recombinations in Sample 2 are between electrons occupying the AlAs  $X_z$ -valleys and  $h_1$  holes confined in the GaAs wells. This is supported by the fact that interband transitions in Sample 2 are accompanied by GaAs and AlAs LO phonon replicas. The emission of LO phonons is necessary to satisfy the crystal momentum conservation rule for the  $X_z h_1$  transitions.

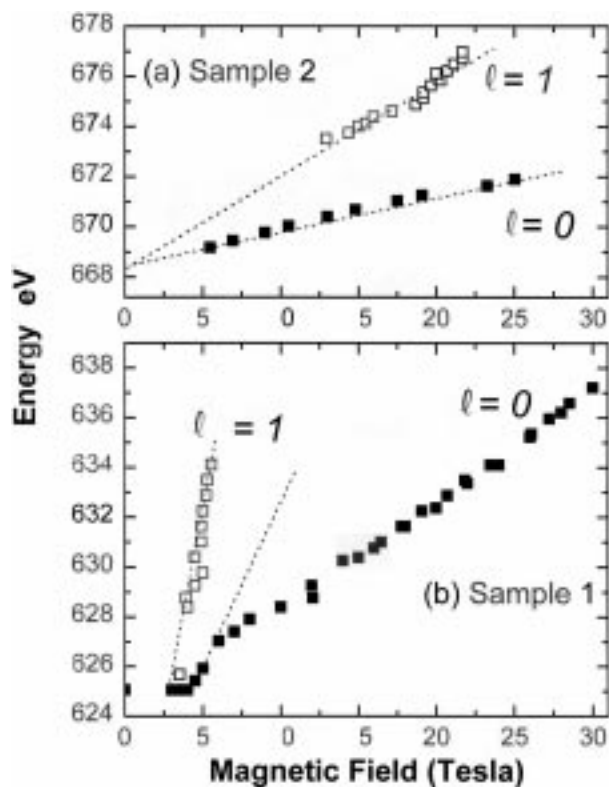


**Figure 1.** Energies of interband Landau transitions plotted as function of applied magnetic field. (a) Sample 2, (b) Sample 1. The energy scale is the same for both graphs. The dotted lines are guides to the eye.

*Reference:*

- <sup>1</sup> Goiran, M., *et al.*, Physica B, **177**, 465 (1992).

## Structural Studies of Chalcogenide Glasses by High Field NMR

Hari, P., Vanderbilt Univ., Physics

Su, T., Univ. of Utah, Physics

Taylor, P.C., Univ. of Utah, Physics

Reyes, A.P., NHMFL

Kuhns, P.L., NHMFL

Moulton, W.G., NHMFL

Sullivan, N.S., NHMFL/UF, Physics

Nuclear Magnetic Resonance (NMR) of  $^{75}\text{As}$  in crystalline and glassy samples of  $\text{As}_2\text{S}_3$  and  $\text{As}_2\text{Se}_3$  has been studied up to 22 T. The results<sup>1,2,3</sup> yield asymmetries in electric field gradient at the As sites. The technique we have developed in mapping out the NMR lineshape at high magnetic fields can be applied to obtain structural information on wide variety of chalcogenide glasses. In this report we summarize the recent measurements on off stoichiometric As-Se glassy composition, Cu-As-Se compounds with variable copper concentrations and two compositions of Cu-In-Se samples. NMR lineshape measurements on off stoichiometric As-Se composition ( $\text{As}_{0.5}\text{Se}_{0.5}$ , stoichiometry corresponds to  $\text{As}_2\text{Se}_3$ ) yield asymmetry parameter values of 0.58 and 0.12 for the two As sites. For Cu-As-Se samples we see progressive broadening of the As NMR lineshape with Cu concentrations (5, 10, and 15% respectively). This is an indication that increasing Cu concentrations causes As sites to become distorted. We also studied two different stoichiometry of Cu-Se-In compositions ( $\text{Cu}_3\text{In}_7\text{Se}_{12}$  and  $\text{Cu}_1\text{In}_1\text{Se}_2$ ). Analysis of the As NMR lineshape on these compounds indicate that they are very nearly axially symmetric (asymmetric parameter is zero). By fitting the experimental lineshape with a theoretical calculation,<sup>3</sup> we obtained the coupling constant for  $\text{Cu}_3\text{In}_7\text{Se}_{12}$  as 107 MHz and for  $\text{Cu}_1\text{In}_1\text{Se}_2$  as 15 MHz. These results indicate that this technique can be useful in many other solids that contain one of the twenty elements whose nuclei have spin 3/2 and relatively large quadrupole moment.

## References:

- 1 Hari, P., *et al.*, Solid State Comm., **104**, 669 (1997).
- 2 Hari, P., *et al.*, J. Non.-Cryst. Solids, **230**, 770 (1998).
- 3 Hari, P., *et al.*, to be published.

# Quantum Hall Effect in InSb

Hicks, J.L., Univ. of Oklahoma, Physics and Astronomy

Murphy, S.Q., Univ. of Oklahoma, Physics and Astronomy

Santos, M.B., Univ. of Oklahoma, Physics and Astronomy

To date, the fractional quantum Hall effect (FQHE) has been observed only in GaAs- and Si-based two-dimensional electronic systems (2DESs). Until our measurements at the NHMFL, all 2DESs in alternative materials either had high densities that pushed the extreme quantum limit to unattainably high magnetic fields or became insulating at  $\nu < 1$ . At first glance, InSb 2DESs appear to be poor candidates for observing the FQHE as this effect is inherently due to electron-electron interactions. The small effective mass ( $0.015m_0$ ) and large dielectric constant ( $18\epsilon_0$ ) of InSb make the ratio of the electron-electron interaction to the Fermi energy rather small.

Nevertheless, our measurements of InSb 2DESs revealed interesting features in the FQH regime.<sup>1</sup> Hall and longitudinal resistances are shown in Figure 1. Although the position of the broad minimum at  $\sim 14$  T is far from  $\nu = 2/3$  and shifts with temperature, this feature may still be due to the  $\nu = 2/3$  FQHE in an inhomogeneous sample. Local areas of different electron density would exhibit the  $\nu = 2/3$  FQHE at different magnetic fields and with different activation energies. Since electron transport will occur through all areas simultaneously, one may observe a broad minimum with a position and temperature dependence that depends on the details of the inhomogeneity. If this is the case, improved sample quality should enable study of the FQHE in InSb. These studies will be most intriguing due to the weak electron correlations and low level of Landau-level mixing in InSb.

An even more unusual situation exists if the broad minimum at  $\sim 14$  T is not the  $\nu = 2/3$  FQH state. The temperature insensitivity of the longitudinal resistance at  $1/2 < \nu < 2/3$  indicates that the 2DES has not entered an insulating phase. According to the theoretical global phase diagram of the QHE<sup>2</sup> and experiments on GaAs 2DESs that cover a wide range of sample quality,<sup>3</sup> all 2DESs should either exhibit the  $\nu = 2/3$  FQHE or become insulating before reaching  $\nu = 1/2$ . Our preliminary result would imply that InSb 2DESs behave differently than GaAs 2DESs and in a way unaccounted for by existing theory. Clearly, more experiments are required to test whether disorder or an intrinsic property of InSb is responsible for our observations in the FQH regime. In either case, the low density and low disorder in our InSb 2DESs provide a unique setting for experiments in the extreme quantum limit.

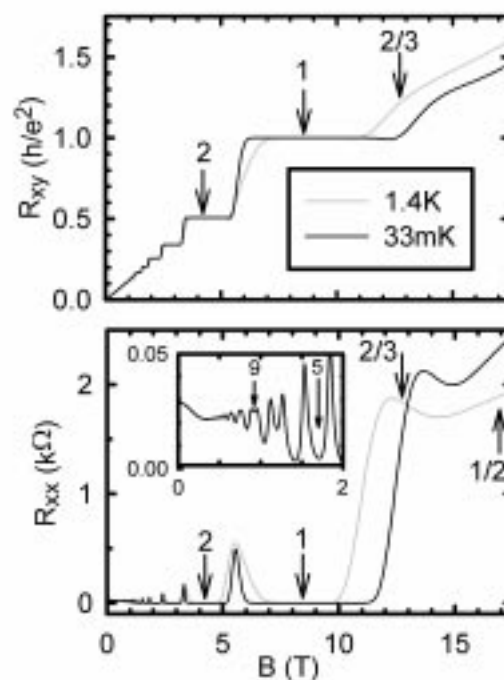


**Figure 1.** Hall and longitudinal resistances of an InSb 2DES with density and mobility of  $2.0 \times 10^{11} \text{ cm}^{-2}$  and  $130,000 \text{ cm}^2 \text{ V}^{-1} \text{ s}^{-1}$ , respectively. Some filling factors are indicated by arrows. Inset: Low-field longitudinal resistance.

## References:

- 1 Goldammer, K.J., *et al.*, accepted by J. Cryst. Growth.
- 2 Kivelson, S.A., *et al.*, Phys. Rev. B, **46**, 2223 (1992).
- 3 Shahar, D., *et al.*, Phys. Rev. Lett., **74**, 4511 (1995).

## Localized Versus Extended States in InGaAsN Photovoltaic Materials

Jones, E.D., Sandia National Laboratories  
 Modine, N.A., Sandia National Laboratories  
 Allerman, A., Sandia National Laboratories  
 Kurtz, S.R., Sandia National Laboratories  
 Wright, A.F., Sandia National Laboratories  
 Tozer, S.W., NHMFL  
 Wei, X., NHMFL

A new semiconductor alloy system, InGaAsN, has been identified as a key candidate material for multi-junction solar cells with efficiencies greater than 40%. The introduction of small amounts of nitrogen (~2%) in the InGaAs alloy system greatly reduces the band gap energy, with reductions approaching 0.5 eV! With the appropriate ratio of indium to nitrogen concentrations, InGaAsN can be lattice matched to GaAs. Lattice matching allows the design of multi-junction cells without the inherent problems found in strained cells. The initial portion of this research program is thus

aimed at understanding the fundamental nature of the effect of adding substitutional isoelectronic nitrogen atoms for arsenic.

A series of InGaAsN alloys with varying nitrogen concentrations with the indium content adjusted to provide lattice matched conditions were grown using metal organic chemical vapor deposition (MOCVD) reactors. In the first study we investigated the photoluminescence energy and line shape for varying growth conditions. Because of the importance and emphasis on materials exhibiting 1 eV band gap energies, we found that nitrogen and indium concentrations of about 2% and 6% respectively, gave the desired results, i.e., correct band gap energy and lattice matched conditions. Studies of the photoluminescence line width and intensity for these samples were performed in order to determine the optimum growth parameters and conditions. Significant increase in the photoluminescence intensity was observed from these samples following a post-growth anneal. A 4-K photoluminescence spectrum is shown in Figure 1. The 4-K band gap energy is about 1150 meV and at 300 K, the band gap energy decreases to about 1100 meV. In order to

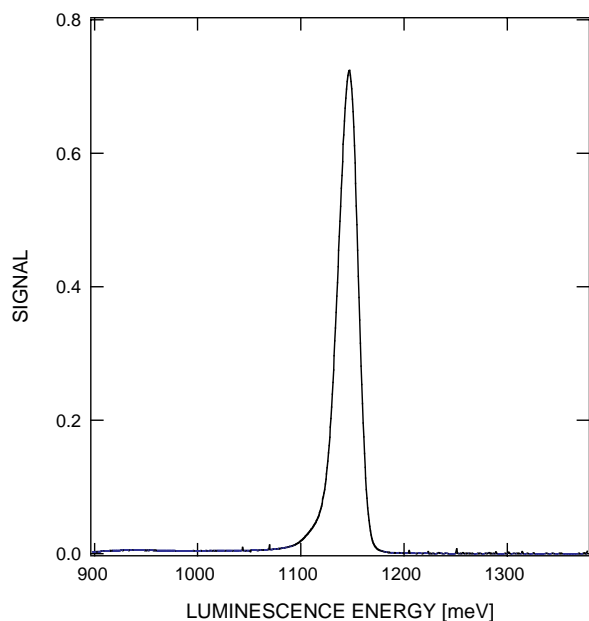


**Figure 1.** Low temperature (4 K) photoluminescence spectrum for an  $\text{In}_{0.06}\text{Ga}_{0.94}\text{As}_{0.98}\text{N}_{0.02}$  epilayer film lattice matched to GaAs. The band gap energy is 1150 meV and the full-width-at-half-maximum is about 22 meV.

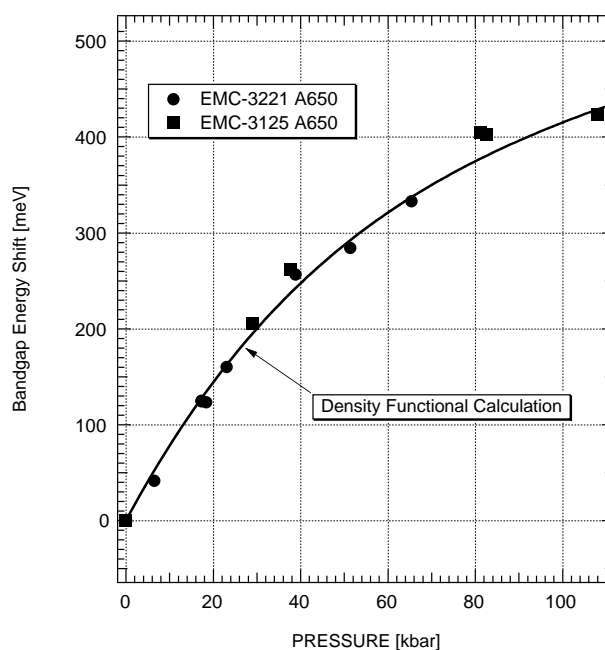


**Figure 2.** Experimental and theoretical comparisons of the change in the low temperature band gap energy vs. pressure.

differentiate impurity from band-to-band luminescence transitions, low temperature (4 K) photoluminescence studies were made as a function of pressure. The pressure dependence of the band gap energy between ambient and 108 kbar is shown in Figure 2. A miniature diamond anvil cell with a methanol/ethanol/water pressure medium in the ratio of 16/3/1 was used to generate the pressure. Also shown in the figure is a theoretical calculation for the change in band gap energy dependence of the lowest energy conduction band using a first principle local density approximation to density functional for 2% nitrogen in GaAsN. The agreement between theory and experiment is surprisingly excellent, considering that theoretical refinements to the calculation are necessary, i.e., addition of indium, etc. The pressure results shown in Figure 2, however, indicate band-to-band and not impurity behavior.

## High Field Magneto-Photoluminescence in Magnetic Semiconductors

Kim, Y., NHMFL/LANL

Wei, X., NHMFL

Schmiedel, T., NHMFL

Dobrowolska, M., Univ. of Notre Dame, Physics

Furdyna, J.K., Univ. of Notre Dame, Physics

Exploratory high field photoluminescence experiments were carried out on II-VI-based magnetic semiconductor alloys ( $\text{Zn}_{1-x}\text{Mn}_x\text{Se}$ ) in the form of epitaxial layers, and on ZnSe/MnSe superlattices. The interest in magnetic semiconductors (sometimes referred to as diluted magnetic semiconductors, or DMSs) arises from the fact that band electrons in these materials, interact with magnetic moments via exchange interactions, leading to enormous Zeeman splitting, several orders of magnitude larger than in ordinary semiconductors. Thus effects associated with spins, normally ignored in semiconductors, become of major importance and lead to entirely new effects.<sup>1</sup>

When the concentration of magnetic ions (Mn in the example of the DMS alloy given above) is low, the giant spin splittings saturate at high fields. Our experiments carried out at higher Mn concentrations at the NHMFL, however, indicate that when the Mn concentration exceeds 5 at. % or so, the Zeeman splitting continues to increase with field to values that are a significant fraction of the energy gap itself (exceeding 0.2 eV). A preliminary report of the high field magneto-optic behavior of this material has already been published. We have now extended these measurements to 50 T, using pulsed fields. Even these fields did not reveal any tendency for the Zeeman shift to saturate.

Such enormous magnetic-field-induced changes in the semiconductor band structure are especially important in the context of magnetic/non-magnetic quantum wells and superlattices, since they can be used to magnetically “tune” the band offset in such heterostructures. Magnetic-field tuning of this kind in turn leads to the observation of entirely new physical phenomena, such as spatial spin segregation, conversion of type-I band alignment into type-II, and control of electron and hole localization by the applied magnetic field.<sup>3,4</sup>

In addition to the enormous size of the Zeeman splittings and the effects that follow, the above high field results shed important light on the nature of magnetism in DMSs and their heterostructures. Magnetic properties of these materials are determined by antiferromagnetic super-exchange interactions between Mn ions. At normal magnetic fields, this Mn-Mn exchange is essentially fixed, and that is why magnetization (and the effects that depend upon it, like the Zeeman splitting referred to above) saturates. The fact that in the present experiments performed on specimens with higher Mn concentrations we do not observe such saturation effects (i.e., that the magnetization continues to grow indefinitely with increasing field) is ascribed to the competition of the applied field with Mn-Mn exchange forces that occurs when the field is sufficiently strong. Such dependence of magnetization on the applied field provides direct

clues toward the understanding of the superexchange process itself.

In addition to the experiments carried out on the Zeeman shift displayed by ZnMnSe alloys in epitaxial layer form, we also have studied the intensity dependence of exciton photoluminescence on the applied field in the high field regime. These experiments were motivated by earlier experiments carried out at lower magnetic fields, where we had already observed—simultaneously with the Zeeman shift—an enormous increase in the intensity of the photoluminescence with increasing field. Although this effect is extremely strong (the intensity increases by one to two orders of magnitude over its zero-field value), the mechanism of this increase is not understood. Our high field experiments at NHMFL-Tallahassee and pulsed field experiments at NHMFL-Los Alamos, involving simultaneous measurement of photoluminescence of the band-edge excitons and of intra-Mn emission, provided a clear indication of a connection between these two radiative channels. This is an important clue, that will be followed in future experiments with the view of understanding the mechanism for the enormous increase in photoluminescence intensity induced by an applied magnetic field.

#### References:

- <sup>1</sup> Furdyna, J.K., *J. Appl. Phys.*, **64**, r29 (1988).
- <sup>2</sup> Schmiedel, T., *et al.*, *Proc. 12th Int. Conf. on Applications of High Magnetic Fields in Semiconductor Physics* (in press).
- <sup>3</sup> Dobrowolska, M., *et al.*, *J. Luminescence*, **60-61**, 308 (1994).
- <sup>4</sup> Dobrowolska, M., *et al.*, *Acta Phys. Polon. A*, **87**, 95 (1995).

## Studies of Magnetic Field Induced New Bound States at the $\nu=2$ and $\nu=1$ Quantum Hall States in GaAs/AlGaAs Single Heterojunctions

Kim, Y., NHMFL/LANL

Rickel, D.G., NHMFL/LANL

Munteanu, F.M., NHMFL/LANL and Northeastern University, Physics

Perry, C.H., Northeastern University, Physics

Simmons, J.A., Sandia National Laboratory

We have investigated the magnetophotoluminescence (MPL) of GaAs/AlGaAs single heterojunctions (SHJ) in high magnetic fields, using a newly commissioned 60 T quasi-continuous (QC) magnet. Highly doped ( $n > 6 \times 10^{11} \text{cm}^{-2}$ ) samples show strong discontinuities in the optical transition energies near the filling factors  $\nu=2$  and 1. We interpret the MPL transition energy reduction, and large intensity changes at these filling factors, as evidence of a valence hole phase transition, from a free state to a spatially localized state due to changes in the many-body interactions between the confined electrons and the dynamic holes.

Our self-consistent calculation for a single heterojunction with 2DEG density of  $6.6 \times 10^{11} \text{cm}^{-2}$  shows that the energy separation, between the Fermi energy of the first subband (E0) and empty second subband (E1), is less than 1 meV. Strong Coulomb interaction between the E0 Fermi energy and the E1 subband, due to their energetic proximity, enhances E1-hole exciton transitions.<sup>1</sup> Consequently, the MPL transition intensity shows Shubnikov-de Haas type oscillations at low fields where the Landau filling factor  $\nu$  is bigger than 2 (see Figure 1 (a)). At around  $\nu=2$ , however, the E1 exciton transition suddenly loses its intensity, and a new peak emerges that is 10 meV below the E1 exciton energy. More surprisingly, another similar transition comes out at  $\nu=1$ .

We interpret these new transitions as formation of new bound states as a consequence of the movement of the dynamic holes in the valence band. In a single heterojunction, holes are not confined and they tend to move to the GaAs flat-band region at low fields, because the Coulomb attraction, between screened electron holes, is smaller than the repulsion between positive donors and holes. As the magnetic field increases, screening between electron holes disappears at  $\nu=2$ , holes move back to the interface, and form a new bound state. The formation of this new bound state, at  $\nu=2$ , is a free state to a Mott type transition.<sup>2</sup> In the higher field, at  $\nu=1$ , where metal-insulator transition occurs, the screening is greatly reduced, and a new phase transition occurs once again. Hence, the new bound state transition, at  $\nu=1$ , is due to an Anderson type localization.<sup>3</sup>

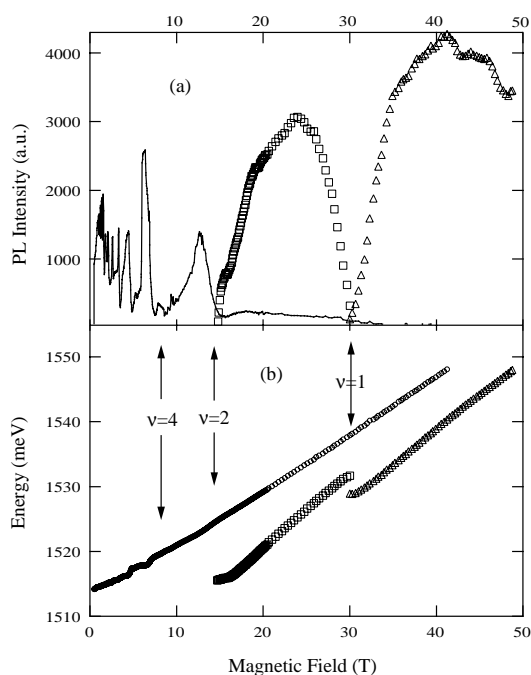


**Figure 1.** PL intensity (a) and transition energy (b) vs. magnetic field. E1 subband PL intensity (circle) shows oscillatory behavior below 15 T. It loses its intensity, however, and new peaks emerge at around 15 T and 30 T due to hole localization.

#### References:

- 1 Kim, Y., *et al.*, Phys. Rev. B. (*in press*).
- 2 Yoon, H.W., *et al.*, Solid Stat. Comm., **287**, 104-5 (1987).
- 3 Anderson, P.W., Phys. Rev., **109**, 1498 (1958).

## High Field Photoluminescence Spectroscopy of the Charged and Neutral Excitons in GaAs Quantum Wells

Lee, K.S., ETRI, Korea  
Kim, Y., NHMFL/LANL

We have studied the high field photoluminescence (PL) spectroscopy of the charged and neutral excitons in GaAs multiple quantum wells (QW) of different well sizes. The sample studied in this work consists of four 30, 19, 12, and 8 nm GaAs quantum wells separated by barriers of 15 nm (Al, Ga)As, and finally, a cap of 60 nm GaAs. Because the effective mass of an electron is lighter than that of a heavy-hole, the tunneling time of the electron, from a narrow to an adjacent wide well, is shorter than that of the heavy hole, resulting in a charge imbalance in each well. Therefore, an excess electron resides in a wide well and is bound to a neutral exciton ( $X^0$ ) to form a negatively charged exciton ( $X^-$ ), while an excess hole in a narrow well is bound to  $X$  to form a positively charged exciton ( $X^+$ ). As the radiative lifetime of a charged exciton is  $\sim 100$  ps<sup>1</sup>, much faster than that of  $X^0$ , which is in the order of  $\sim 10$  ns, a slight charge imbalance can give rise to a pronounced PL peak associated with the charged exciton.

Figure 1 shows a series of PL spectra taken at 4 K in the presence of quasi-continuous  $B_{\perp}$  fields from 0 T to 58 T, with 1 T steps. Two PL peaks of the zero-field spectrum, at 1.514 eV and 1.517 eV, are associated with the free exciton peaks in bulk GaAs and the exciton ground state in the 60 nm GaAs cap, respectively. Other features at 1.519 eV, 1.526 eV, 1.538 eV, and 1.562 eV, originating from the four QWs of well sizes 30, 19, 12, and 8 nm, respectively, actually consist of two peaks associated with the charged and neutral excitons, whose intensities reveal the opposite oscillatory behaviors with the magnetic field. From circular polarization measurements on the double peaks, we found  $X^-$  in the 30 nm and the 19 nm QWs, and  $X^+$  in the other two wells. Oscillations

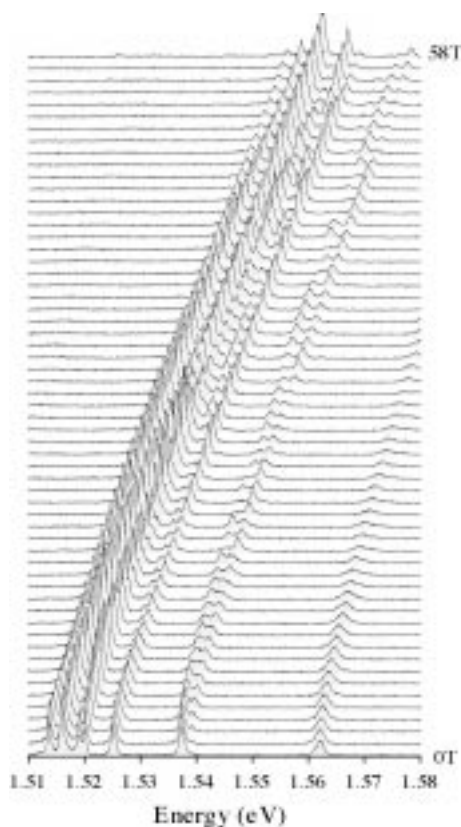


**Figure 1.** A series of PL spectra of the GaAs quantum wells in the presence of  $B_{\perp}$  fields from 0 T to 58 T with 1 T steps.

in the PL intensities of the charged and neutral excitons may be understood with the modulation of the density of excess carriers by a magnetic field, which gives some effects on carrier dynamics in the PL processes, consisting of absorption, relaxation, tunneling, exciton formation, and radiative recombination. The charged and neutral exciton showed the similar oscillatory behaviors in the presence of in-plane magnetic fields ( $B_{\parallel}$ ). Further studies are definitely needed, however, for a better understanding of our findings.

*Reference:*

- <sup>1</sup> Finkelstein, G., *et al.*, Phys. Rev. B, **58**, 12637 (1998).

## Discontinuous Red-Shift in the Emission Spectrum of a Two-Dimensional Electron Gas

Lee, X.Y., Univ. of California-Los Angeles (UCLA),  
Physics and Astronomy  
Jiang, H.W., UCLA, Physics and Astronomy  
Kim, Y., NHMFL/LANL  
Schaff, W., Cornell Univ., Electrical Engineering

Lately, there has been a surge of theoretical and experimental efforts in trying to understand the photoluminescence spectra of two dimensional electron gas (2DEG) at integral Landau level filling factors. We have studied spin-resolved photoluminescence of a high-density GaAs/AlGaAs heterostructure up to 60 T using the new quasi-continuous magnet at Los Alamos National Laboratory. At a field of 27.5 T, corresponding to a filling factor of  $\nu=2$  of the 2DEG, we find that the dominant Fermi-edge-enhanced emission line disappears abruptly, and an anomalous luminescence line emerges concurrently with a red-shift of about 10 meV.

In the literature, red-shift in energy observed in some systems has been explained by the model that

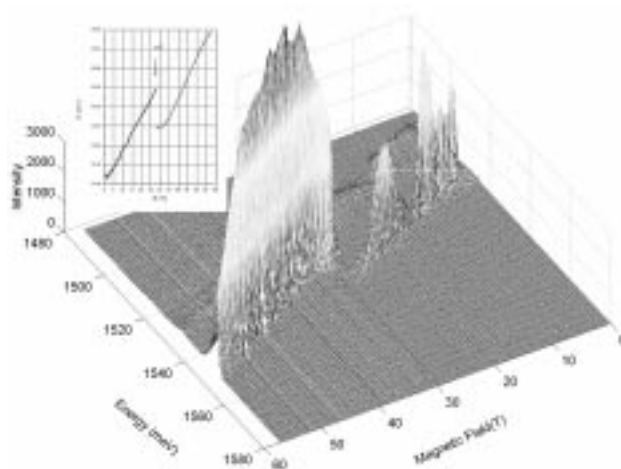


**Figure 1.** Photoluminescence spectra of the high-density  $n = 1.34 \times 10^{12} / \text{cm}^2$  GaAs/AlGaAs heterostructure at a bath temperature of 450 mK in a 3D plot. Inset photon energy as a function of magnetic field.

there are two distinct ground states for the final-state excitations of the recombination across an integer-filling factor. The discontinuity seen in our experiment is, however, much larger (about a factor of ten) than those predicted by theories, and previously reported. Our data therefore can be interpreted by the existing theories.

We have proposed a simple, yet revealing, model to explain our observations as a magnetic-field-induced phase transition from a free state to a spatially localized bound state at  $\nu=2$ . This transition, much like the Mott transition, is a consequence of the competition between the build-in repulsive potential of the heterostructure, and the attractive potential of the electrons. It is driven by a strong reduction of the screening strength of a 2DEG in high magnetic fields.

## Spin-Resolved Photoluminescence Probe of Two-Dimensional Holes in a p-Type GaAs/AlGaAs Heterostructure

Lee, X.Y., Univ. of California-Los Angeles (UCLA),  
Physics and Astronomy  
Dultz, S., UCLA, Physics and Astronomy  
Jiang, H.W., UCLA, Physics and Astronomy  
Kim, Y., NHMFL/LANL  
Schaff, W., Cornell Univ., Electrical Engineering

Recently, a metal to insulator transition has been found in two-dimensional holes in p-type GaAs/AlGaAs heterostructures at zero magnetic fields. The 2D holes system is particularly interesting due to its large ratio of the correlation energy to the kinetic energy. It has been proposed that the insulating phase at  $B = 0$  is a Wigner solid phase (or glass phase in the presence of disorder).

In an attempt to establish a connection between the zero-field insulating phase and the more well-established high-field Wigner solid phase, we

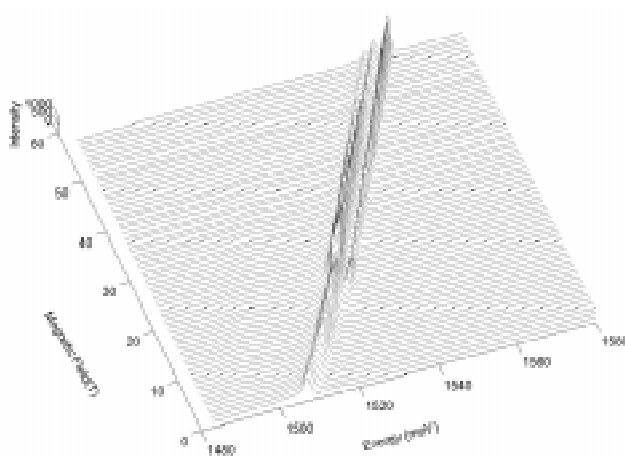


**Figure 1.** An overhead view of the photoluminescence spectra of the 2D hole gas single heterostructure in the  $\sigma^-$  polarization of the emitted light.

have studied photoluminescence energy spectrum of two-dimensional holes in a p-type GaAs/AlGaAs single heterostructure, by using the newly commissioned quasi-continuous magnet at LANL. The spectroscopy was done in both the  $\sigma^+$  and  $\sigma^-$  circular polarizations for magnetic fields up to 60 T.

At low magnetic fields, the emission spectrum was dominated by the so-called H-band line that was due to the recombination of a photo-excited electron, with a hole confined near the heterostructure interface. At Landau level filling factor  $\nu < 1.3$ , a new high energy line, with a very narrow line-width, emerged. Unlike the H-band line, the new line was strongly polarization dependent. In the high-field insulating phase for  $\nu < 0.6$ , the spectrum was dominated by the new high-energy line. Furthermore, another low-energy line (at energy even lower than that of the H-band line) appeared.

The observed spectra are very different from that given by the two-dimensional electron systems, and that reported for the low-density 2D hole systems. Further studies are planned to reveal the nature of these high-field luminescence features in the insulating phase.



## Studies of Microwave Resonance in Two-Dimensional Hole System at High B



Li, C.-C., Princeton Univ., Physics  
 Engel, L.W., NHMFL  
 Tsui, D.C., Princeton Univ., Physics  
 Shayegan, M., Princeton Univ., Physics

In high quality two-dimensional systems of electrons or of holes, microwave resonances<sup>1,2</sup> have been observed in the insulating phase that terminates fractional quantum Hall effect series at high magnetic fields (B). Since this insulating phase is likely a form of pinned Wigner crystal (WC), it is natural to interpret the resonance as a pinning mode, in which WC domains oscillate in the potential of pinning impurities.

We have performed microwave measurements on high quality two-dimensional hole systems (2DHS), to survey the dependence of the resonance on hole areal density ( $p$ )<sup>3</sup>, temperature (T)<sup>4</sup>, and dc current density ( $j_{dc}$ ).<sup>4</sup> The microwave technique<sup>1</sup> used a metal transmission line that was patterned directly on the top surface of the sample, and coupled to the 2DHS capacitively. The microwave conductivity ( $\text{Re } \sigma_{xx}$ ) was calculated quantitatively from the loss of the transmission line.

The T dependence<sup>4</sup> of the resonance features is gradual, and so is suggestive of a continuous melting transition of a WC as T is raised. We examined the T dependence of the resonance in a sample with hole density  $p = 5.4 \times 10^{10} \text{ cm}^{-2}$ , at  $B = 13 \text{ T}$ . At low T, the resonance is strikingly sharp, and the resonance Q (full width at half maximum divided by peak frequency) is about 5. Increasing T broadens the resonance and reduces the peak  $\text{Re } \sigma_{xx}$  so that the resonance becomes indistinguishable above about 230 mK. As T is increased above 100 mK, the peak frequency ( $f_{pk}$ ) shifts downward only slightly from its low T value of 1.25 GHz.

We have performed studies<sup>3</sup> of the resonance as the hole density ( $p$ ) is reduced by means of a backgate bias. In one sample  $f_{pk}$  increases rapidly from 1.25 GHz at the zero bias density of  $p = 5.4 \times 10^{10} \text{ cm}^{-2}$ , to 3.7 GHz by  $p = 1.6 \times 10^{10} \text{ cm}^{-2}$ , while the resonance remains well-defined. Interpretation of the decreasing  $f_{pk}$  vs.  $p$ , in terms of a pinned WC, requires a “weak pinning” model, in which domain size (L) is determined by a balance between the carrier-carrier interaction and carrier-impurity interaction energies, and in which L increases with increasing  $p$ .

For a sample of density  $p = 4.3 \times 10^{10}$ , at  $B = 13 \text{ T}$ , we applied a dc bias (V) to two Ohmic contacts, and simultaneously obtained microwave spectra.<sup>4</sup> The contacts were arranged to inject current through the area of 2DHS that is within the microwave transmission line. The I-V characteristic exhibited a clear threshold. The current density ( $j_{dc}$ ) was estimated as total current divided by the sample width. Surprisingly, the resonance remained prominent for V well beyond threshold, and over several orders of magnitude in  $j_{dc}$ , up to  $j_{dc} \sim 3 \text{ nA/mm}$ . The peak broadens and its height is reduced as  $j_{dc}$  increases.  $f_{pk}$  and the integrated  $\text{Re } \sigma_{xx}$  vs.  $f$  both remain constant with  $j_{dc}$  up to about 300 pA/mm, though they decrease at higher current. The observed effects of dc bias on the resonance could not be distinguished from the dc power heating the sample.

The resonance surviving in a condition where the 2DHS insulator is depinned and carries current may indicate that the current flow is filamentary, and involves only a small part of the sample. On the other hand, the data may not rule out some models involving more spatially uniform flow of the WC, since even at the largest  $j_{dc}$  we applied, the WC washboard frequency<sup>5</sup> (drift velocity/lattice constant) is only around 1 MHz, much less than  $f_{pk}$ .

### References:

- 1 Li, C.-C., *et al.*, Physical Review Letters, **79**, 1353 (1997).
- 2 Andrei, E.Y., *et al.*, Phys. Rev. Lett., **60**, 2765 (1988);

Stormer, H.L., *et al.*, *ibid.*, **62**, 972 (1989); Andrei, E.Y., *et al.*, *ibid.*, **62**, 973 (1989).

<sup>3</sup> Li, C.-C., *et al.*, Physical Review Letters, submitted.

<sup>4</sup> Li, C.-C., *et al.*, to appear in proc. Physical Phenomena at High Magnetic Fields-III.

<sup>5</sup> Li, Y.P., *et al.*, Solid State Commun., **99**, 255 (1996).

## Numerical Studies of Quantum Hall Fluids

Melik-Alaverdian, V., NHMFL

Bonesteel, N.E., NHMFL/FSU, Physics

Ortiz, G., LANL

This goal of this research program is to develop and apply new numerical tools for studying various quantum Hall states and their excitations. Recent accomplishments include (1) a new numerical method for studying composite fermion wave functions projected into the lowest Landau level;<sup>1</sup> and (2) fixed-phase diffusion Monte Carlo studies of the effect of Landau level mixing on fractionally charged excitations of the FQHE<sup>2</sup> and on the so-called skyrmion excitations of the IQHE.<sup>3</sup>

More recently, in collaboration with J.K. Jain and K. Park at Pennsylvania State University, a new numerical technique for studying the so-called Pfaffian wave function was developed and used to study the stability of this state. It was shown that for Landau level filling factor  $\nu=1/2$  the incompressible Pfaffian can be stabilized over the compressible composite Fermi sea if the short-range part of the electron-electron interaction is softened by increasing the “width” of the two dimensional electron gas. The results of this study also showed that the Pfaffian is stable for  $\nu=5/2$  and is spin-polarized, even in the absence of Zeeman coupling—a result consistent with the experimental observation of an incompressible FQHE state at  $\nu=5/2$  as well as the growing consensus that this state is spin polarized.

### References:

<sup>1</sup> Melik-Alaverdian, V., *et al.*, Phys. Rev. B, **58**, 1451(1998).

<sup>2</sup> Melik-Alaverdian, *et al.*, Physica E, **1**, 138 (1997).

<sup>3</sup> Melik-Alaverdian, V., *et al.*, preprint.

<sup>4</sup> Park, K., *et al.*, Phys. Rev. B, **58**, 10167 (1998).

## Magnetic Field Induced Charged Exciton Studies in a GaAs/AlGaAs Single Heterojunction

Munteanu, F.M., NHMFL/LANL and Northeastern University, Physics

Kim, Y., NHMFL/LANL

Perry, C.H., NHMFL/LANL and Northeastern University, Physics

Rickel, D.G., NHMFL/LANL

Simmons, J.A., Sandia National Laboratory

Reno, J.L., Sandia National Laboratory

Over the last few years, the negatively and positively charged magneto-excitons ( $X^-$  and  $X^+$ ) have received renewed attention because of their enhanced binding energy in quasi-two-dimensional semiconductors, almost ten times higher than in a 3-D system. One theoretical study indicates that quasi-2D systems, which approximate to a biplanar system (e.g. heterojunctions), are most unlikely to exhibit PL effects due to the charged excitons.

We report here the results of photoluminescence (PL) measurements on a very high mobility ( $m>3\times10^6\text{ cm}^2/\text{Vs}$ ), low modulation-doped GaAs/ $\text{Al}_{0.3}\text{Ga}_{0.7}\text{As}$ , single heterojunction. The polarized spectra show clear evidence of the singlet and triplet states of  $X^-$  that are formed at high magnetic fields, at  $\nu < 1$ . Figure 1 plots  $s^+$  polarized (right circularly polarized) and  $s^-$  polarized (left circularly polarized) PL spectra for an applied magnetic field of 17 T. The two supplementary peaks in  $s^+$  polarization are, in our interpretation, the optical signature of the singlet ( $X^-_s$ ) and triplet ( $X^-_t$ ) states of  $X^-$ . The inset of Figure 1 shows the variation of the energies of  $X^-_s$  and  $X^-_t$  relative to that of the neutral exciton  $X^0$  as a function of magnetic field.

It is important to notice that the peaks corresponding to  $X^-_s$  and  $X^-_t$  *do not cross*. This contradicts the general belief that at very high fields the triplet state, in accordance with Hund's rules,

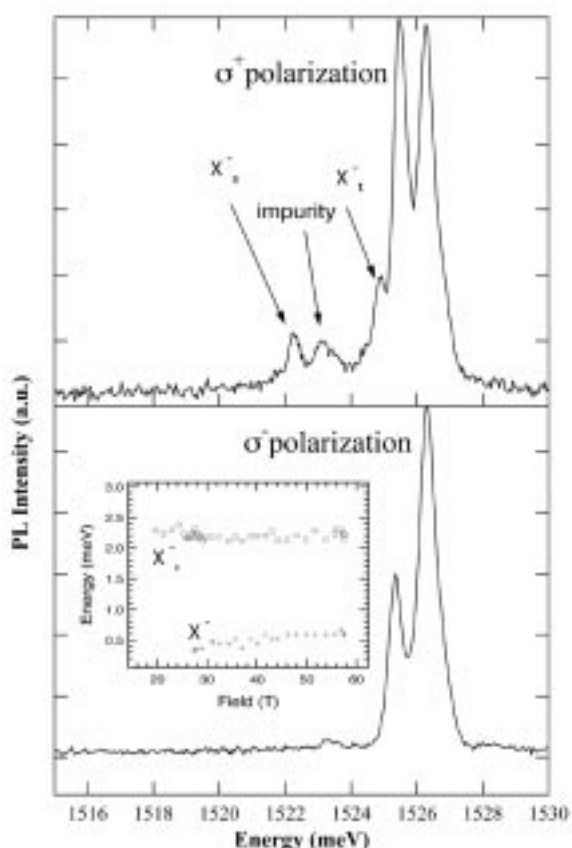


**Figure 1.** Right and left circularly polarized spectra at 17 T. The inset shows the differences of the energies of the charged excitons with respect to the energy of the neutral exciton as a function of magnetic field.

should become the ground state, but is in good agreement with more complete calculations that take into consideration both higher Landau levels and higher energy subbands, and predict the non-crossing behavior for fields up to 50 T in the case of a large quantum well. Another important thing is that, while the energy of  $X_t$  state relative to neutral exciton increases with field, the energy of the  $X_s$  state is almost constant. This behavior is determined by the larger spatial extent of the  $X_t$  state compared with that of the  $X_s$  state, so that an increase of the magnetic field will affect the former one to a larger degree. It must be noticed the good agreement between the values of these energies and other published data.

## Oscillatory Cyclotron Resonance Effective Mass in $\text{ZnSe}/\text{Zn}_{1-x-y}\text{Cd}_x\text{Mn}_y\text{Se}$ Heterostructures

NHMFL

Ng, H.K., FSU, Physics and MARTECH  
Storr, K., FSU, Physics and MARTECH  
Smorchkova, I.P., Pennsylvania State Univ., Physics  
Samarth, N., Pennsylvania State Univ., Physics

Two-dimensional electron gas (2DEG) structures based on modulation doped  $\text{ZnSe}/\text{Zn}_{1-x-y}\text{Cd}_x\text{Mn}_y\text{Se}$  single quantum wells show novel spin-dependent effects in both diffusive and quantum transport (PRL 78, 3571 (1997), PRB 58, R4238 (1998)). Here, we report on the first measurements of cyclotron resonance (CR) and effective mass in such magnetic 2DEG samples. Far-infrared absorption measurements are carried out at 4.2 K on samples with carrier densities around  $4 \times 10^{11} \text{ cm}^{-2}$ , revealing a clear CR peak in magnetic fields ranging from 5 T to 30 T. While the CR frequency shows the expected linear variation with magnetic field in non-magnetic control samples, the magnetic 2DEGs exhibit clear deviations from linearity in the vicinity of the  $\nu = 2$  and  $\nu = 1$  filling factors (Figure 1). Beyond  $\nu = 1$ , the data

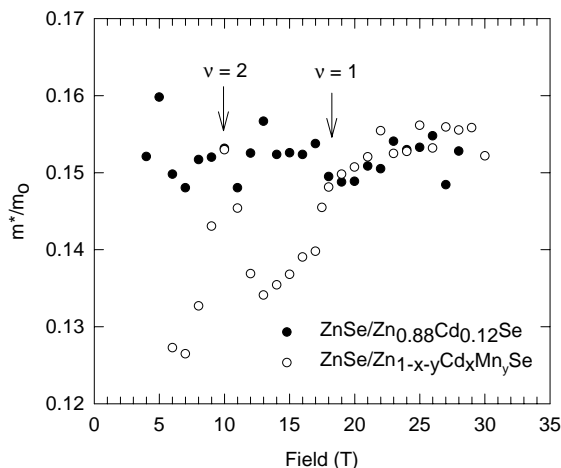


**Figure 1.** Ratio of the effective mass over free electron mass for the non-magnetic (solid circles) and magnetic (open circles) 2DEG. Note the dramatic change in the ratio at half-filling factors for the magnetic case.

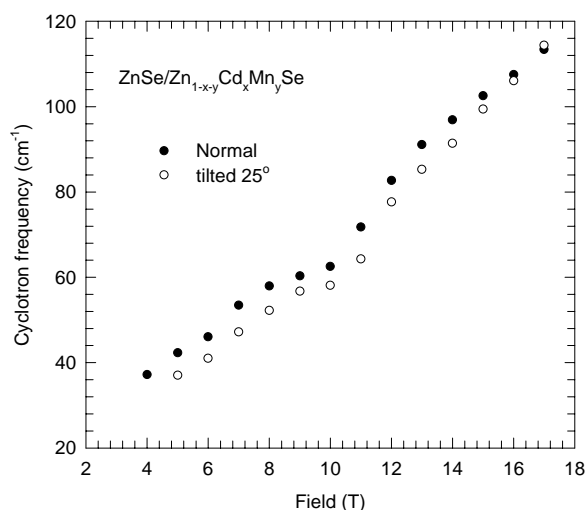


**Figure 2.** The 2DEG tends toward 3D characteristics as the magnetic field approaches 17 T.

for the magnetic and non-magnetic 2DEGs become indistinguishable, corresponding to an effective mass of  $0.152 \pm 0.005 m_0$ . At half-filling the effective mass is decreased significantly. This is most likely due to the filling-factor dynamic screening of the electron-spin scattering.

Measurements in tilted fields are employed to gain further insights into the oscillatory behavior in the magnetic 2DEGs. Figure 2 shows the comparison of the cyclotron resonance with the magnetic field perpendicular to the sample and tilted at a  $25^\circ$  to the plane of the sample. The figure clearly shows that at low fields the electron gas is in a 2D behavior but as the field is increased the electron tends toward 3D characteristics. This data is been analyzed.

Work at FSU is supported by the Center for Material Research and Technology; work at Pennsylvania State University is supported by ONR grant N00014-97-1-0577 and by NSF-QUEST.

## FQHE at Ultra-Low Temperatures and High Magnetic Fields

Pan, W., Princeton Univ., Physics/NHMFL  
 Xia, J.S., NHMFL/UF, Physics  
 Shvarts, V., NHMFL/UF, Physics  
 Adams, E.D., NHMFL/UF, Physics  
 Stormer, H.L., Columbia Univ., Physics/Lucent Technologies  
 Tsui, D.C., Princeton Univ. Physics  
 Pfeiffer, L.N., Lucent Technologies  
 Baldwin, K.W., Lucent Technologies  
 West, K.W., Lucent Technologies

Three GaAs/Ga<sub>1-x</sub>Al<sub>x</sub>As samples, with various fixed density, were studied at ultra-low temperatures down to 4 mK and high field up to 15 T. The samples, with their 8 contacts directly soldered to separated silver power sintered heat exchangers, were immersed in the liquid <sup>3</sup>He, which was cooled by a powerful 5 mole PrNi<sub>5</sub> nuclear stage refrigerator recently built at the University of Florida. The data analysis shows that the two-dimensional electron system (2DES) was successfully cooled down to 4 mK with liquid <sup>3</sup>He bath being around 2.5 mK.

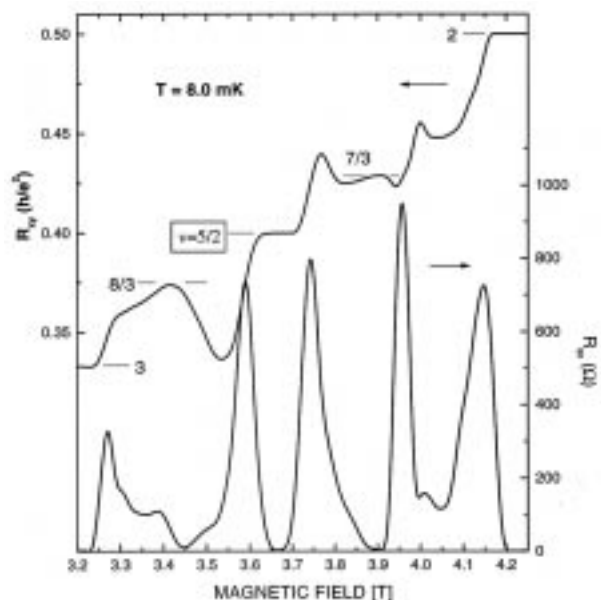


**Figure 1.** FQHE in GaAs/Ga<sub>1-x</sub>Al<sub>x</sub>As at  $\nu=5/2$ .

For the sample with density  $n = 2.3 \times 10^{11} / \text{cm}^2$  and mobility  $\mu = 1.4 \times 10^7 \text{ cm}^2/\text{Vs}$ , Figure 1 shows a vanishing  $R_{xx}$  at  $\nu=5/2$ <sup>[1]</sup> and, for the first time, a precisely quantized Hall resistance  $R_{xy}$  to the value of  $2h/5e^2$  in the magnetic field range between 3.63 T and 3.70 T at  $T = 8.0 \text{ mK}$ . The activation energy gap  $\Delta$  at  $\nu=5/2$ , defined by  $R_{xx} \sim \exp(-\Delta/T)$ , was found to be 54.0 mK. The activation energy at other FQHE states,  $\nu=7/3$  and  $\nu=8/3$ , were also measured and found to be very similar to the activation energy at  $\nu=5/2$  within our experimental error. The experimental details and more data will be published in elsewhere.

#### Reference:

- 1 Willett, R.L., *et al.*, Phys. Rev. Lett., **59**, 1776 (1987).

## The Effective Mass and its Density Dependence of Composite Fermions with Four Flux Quanta

Pan, W., Princeton Univ., Physics/NHMFL  
 Yeh, A.S., Princeton Univ., Physics/NEC  
 Stormer, H.L., Columbia Univ., Physics/Bell Labs  
 Tsui, D.C., Princeton Univ., Electrical Eng.  
 Pfeiffer, L.N., Bell Labs  
 Baldwin, K.W., Bell Labs  
 West, K.W., Bell Labs

The composite fermion (CF) model<sup>1</sup> has been very successful in interpreting the fractional quantum Hall effect (FQHE) features of a two-dimensional electron system (2DES) around Landau level filling factor  $\nu = 1/2$  and  $3/2$ . In the past years, experiments have demonstrated the existence of a well-defined Fermi wave factor and the associated effective mass for <sup>2</sup>CFs (the CFs at  $\nu = 1/2$ ). In principle, the CF model should hold at any other even-denominator filling factors besides  $\nu = 1/2$  and  $3/2$ , such as at  $\nu = 1/4$  and  $3/4$  (<sup>4</sup>CF and its particle-hole conjugate) or even at  $\nu = 1/6$  (<sup>6</sup>CF). Little work has been done, however, around the other filling factors, mainly due to the poor

developed FQHE features and the unavoidable formation of insulating phases at high magnetic field.

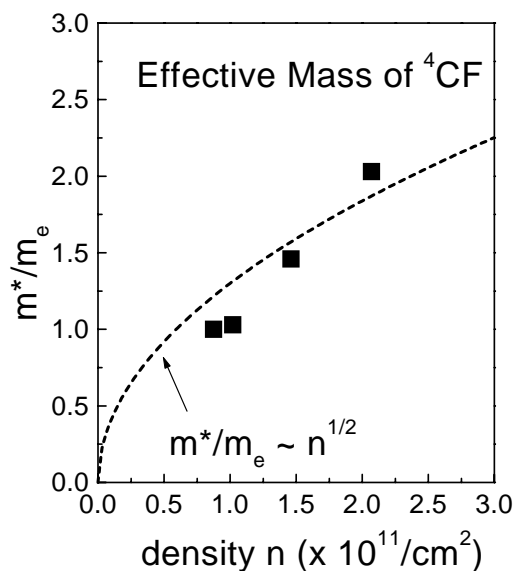


Figure 1. Density dependence of effective mass of <sup>4</sup>CF.

In this report, we present recent data on the effective mass ( $m^*$ ) measurements of <sup>4</sup>CFs in a series of high quality GaAs/AlGaAs heterostructure samples, using the temperature dependence of the Shubnikov-de Haas effect and following the methodology developed in the previous experiments. The experiments were performed either in a superconducting magnet with field up to 18 T and temperature down to 25 mK or a resistive magnet with field up to 33 T and temperature down to 40 mK.

In a sample of density  $n = 0.87 \times 10^{11} / \text{cm}^2$  and mobility  $\mu = 8 \times 10^6 \text{ cm}^2/\text{Vs}$ , for  $\nu > 1/4$ ,  $m^*$  is nearly constant ( $m^* \sim 1.0 m_e$ ,  $m_e$  is the bare electron mass) and scales as  $B^{1/2}$  with the mass derived from data around  $\nu = 1/2$ . A slight increase in  $m^*$  as  $\nu \rightarrow 1/4$  resembles the findings around  $\nu = 1/2$ . For  $\nu < 1/4$ , the mass increases rapidly at a rate that is strongly sample dependent. It is probably a result of the formation of an insulating phase at even higher magnetic field.

By employing a new type of samples—the Heterojunction Insulated Gated Field-Effect Transistors (HIGFETs), the 2DES density can be tuned continuously up to  $7.5 \times 10^{11} / \text{cm}^2$ . For the

first time, we can study the density dependence of the effective mass of  $^4\text{CF}$  in one sample. The effective mass of  $^4\text{CFs}$  obtained at different densities shows considerable deviation from a simple  $B^{1/2}$  relationship, predicted by the CF model. The reason for this discrepancy is presently not clear.

*Reference:*

- <sup>1</sup> *Perspectives in Quantum Hall Effects*, edited by S. Das Sarma and A. Pinczuk, Wiley and Sons (1997).

## Magnetization Measurements on the III-VI Diluted Magnetic Semiconductor $\text{Ga}_{1-x}\text{Mn}_x\text{Se}$ at High Fields

Pekarek, T.M., Univ. of North Florida, Natural Sciences  
 Hughes, S.B., Stanton College Prep., Physics  
 Graf, A.T., Univ. of North Florida, Natural Sciences  
 Lewis, R.S., Univ. of North Florida, Natural Sciences  
 Crooker, B.C., Fordham Univ., Physics  
 Miotkowski, I., Purdue Univ., Physics  
 Ramdas, A.K., Purdue Univ., Physics

These new layered III-VI Diluted Magnetic Semiconductor (DMS) systems (with lower symmetry) complement the enormous progress in the II-VI DMS and the more recent efforts in the Mn doped III-V DMS systems. The III-VI DMS  $\text{Ga}_{1-x}\text{Mn}_x\text{Se}$  exhibits a strong red emission at 1.804 eV attributed to the Mn. GaSe itself is known for its remarkable nonlinear optical properties and is a promising material for photoelectronic applications.

Little is known about the magnetic properties of this new class of layered III-VI DMS except for a single publication<sup>1</sup> that presents magnetization data on  $\text{Ga}_{1-x}\text{Mn}_x\text{Se}$ . Although the Mn ions in  $\text{Ga}_{1-x}\text{Mn}_x\text{Se}$  are tetrahedrally coordinated as in the II-VI DMS, the magnetic behavior is strikingly different from any of the II-VI DMS. In fields up to 6 T at 5 K, the magnetization of  $\text{Ga}_{1-x}\text{Mn}_x\text{Se}$  remains linear with field.<sup>1</sup>

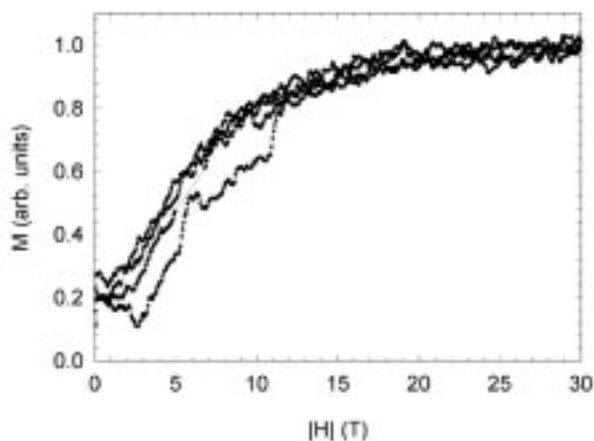


**Figure 1.** Magnetization data vs. the magnitude of the field for  $\text{Ga}_{1-x}\text{Mn}_x\text{Se}$  at 1.5 K in fields between  $\pm 30$  T. The magnetization saturates slower than a standard paramagnet and is reminiscent of Van-Vleck paramagnetism seen in Fe-based II-VI DMS.

Magnetization measurements on  $\text{Ga}_{1-x}\text{Mn}_x\text{Se}$  were made at the NHMFL using the cantilever method. Magnetization data versus the magnitude of the field for  $\text{Ga}_{1-x}\text{Mn}_x\text{Se}$  at 1.5 K in fields between  $\pm 30$  T are shown in Figure 1. Data below  $\pm 2$  T can be ignored due to reduced sensitivity of the cantilever. These data show that the magnetization saturates significantly slower than a standard paramagnet. Theoretical work is underway to investigate the underlying energy levels that give rise to the observed magnetic behavior in this new layered III-VI DMS system.

*Reference:*

- <sup>1</sup> Pekarek, T.M., *et al.*, J. Appl. Phys., **83**, 7243 (1998).

## Measurement of the Hall Scattering Coefficient in 4H-SiC Epitaxial Layers

Rutsch, G., Univ. of Pittsburgh, Physics  
 Devaty, R., Univ. of Pittsburgh, Physics  
 Choyke, W.J., Univ. of Pittsburgh Physics  
 Rowland, L.B., Sterling Semiconductor, VA; formerly  
 with Northrop Grumman Science Center, Pittsburgh  
 Wischmeyer, F., Daimler Benz Research, Frankfurt  
 Niemann, E., Daimler Benz Research, Frankfurt

We are studying the Hall scattering factor as a function of magnetic field in 4H silicon carbide epitaxial layers. The Hall scattering coefficient is a material and field dependent parameter necessary for the extraction of the carrier concentration from measured Hall coefficient data. Theory<sup>1</sup> predicts a saturation at a value of one at high fields. It is known to vary between 0.5 and 2 at low field in other semiconductors, so it is customarily set to one in Hall analysis.

Activation energies extracted from temperature dependent Hall data with the Hall coefficient set to one have been found to be anomalously high, and an influence of the Hall scattering factor was suspected. Experiments in a 9 T superconducting solenoid at the University of Pittsburgh have yielded evidence of saturation of the Hall scattering coefficient at temperatures far below room temperature.<sup>2</sup> The onset of saturation is known to occur when the product of carrier mobility and magnetic field larger than one. Knowledge of the carrier mobility led to the hope of observing saturation in the 30 T magnet at NHMFL. A first trial with one sample has shown that this is indeed the case. Further measurements are in progress.

### References:

- 1 Blood, B. and Orton, J.W., *The Electrical Characterization of Semiconductors: Majority Carriers and and Electron States*, Academic Press Inc, 1992.
- 2 Rutsch, G., *et al.*, JAP, **84**, No 4, 2062-2064 (15 Aug 1998).

## Electrical Conductivity Detection of Nuclear Hyperpolarization: A New Method of Measuring the Zeeman Energy of Two-Dimensional Electrons in GaAs/AlGaAs Quantum Wells

Vitkalov, S.A., UF, Chemistry and P.N. Lebedev  
 Physical Inst.  
 Bowers, C.R., NHMFL/UF, Chemistry  
 Simmons, J.A., Sandia National Laboratories  
 Reno, J.L., Sandia National Laboratories

We have demonstrated that nuclear spin hyperpolarization, induced by microwave dynamic nuclear polarization (DNP) at low temperature, can appreciably change the 2D electron conductivity of GaAs/AlGaAs quantum wells at unity filling in the quantum Hall effect. The longitudinal magnetoconductivity traces (per layer) in the vicinity of the unity filling factor are shown before and after the application of an ESR resonant

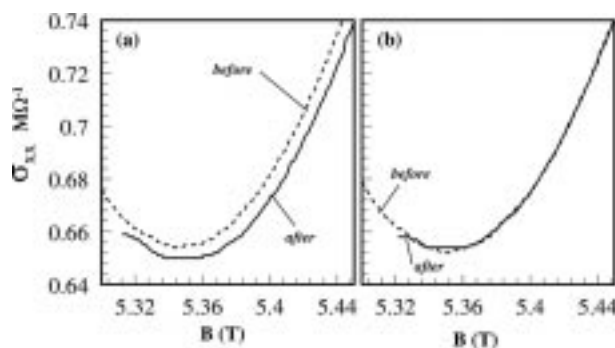


**Figure 1.** Field dependancies of the DC conductivity (per layer) before (dashed curves) and immediately following (solid curves) microwave excitation of sample EA124 during the magnetic field down-sweep at  $T = 2.50$  K in the unity filling regime. In (b), the nuclear spin polarization was enhanced by down-swept microwave DNP. The microwave frequency was 32 GHz, corresponding to  $B = 5.5$  T before DNP. In (a), the same microwave power was applied but at 20.0 GHz, a frequency well outside of the ESR range so that the nuclear polarization cannot be enhanced.

(a) and non-resonant (b) microwave field. The enhanced hyperfine field, which is measured via the Overhauser shift of the electrically detected ESR signal,<sup>1</sup> provides an additional contribution to the electron Zeeman energy that contributes to the activation energy of the conductivity.<sup>2</sup> We have demonstrated that this previously unobserved effect can be used to measure the spin of charged quasiparticle excitations in the quantum Hall Effect at unit filling factor.

#### References:

- <sup>1</sup> Dobers, M., *et al.*, Phys. Rev. Lett., **72**, 1650 (1988).
- <sup>2</sup> Schmeller, A., *et al.*, Phys. Rev. Lett., **75**, 4290 (1995).

## Hyperfine Coupling Between Two-Dimensional Electrons and Quantum Well Nuclei

Vitkalov, S.A., UF, Chemistry and P.N. Lebedev Physical Inst.  
 Bowers, C.R., NHMFL/UF, Chemistry  
 Simmons, J.A., Sandia National Laboratories  
 Reno, J.L., Sandia National Laboratories

We have measured the hyperfine coupling between 2D conduction electrons and nuclei in n-type GaAs/AlGaAs multiquantum wells at unit filling factor in the quantum Hall regime. The hyperfine coupling constant in these systems is simply the constant of proportionality between the Overhauser shift and the nuclear spin polarization. The Overhauser shift was determined via electrically detected ESR<sup>1</sup> immediately following optical excitation of interband transitions with unpolarized light. The inset in the figure shows the ESR signal recorded with increasing delay following the optical pumping period. The main part of the figure shows the decay of the Overhauser shift (solid circles) and the growth (open circles) as a function of the pumping duration. The nuclear polarization under the same conditions was estimated from the enhancement factor of the NMR signal. These results yield a hyperfine

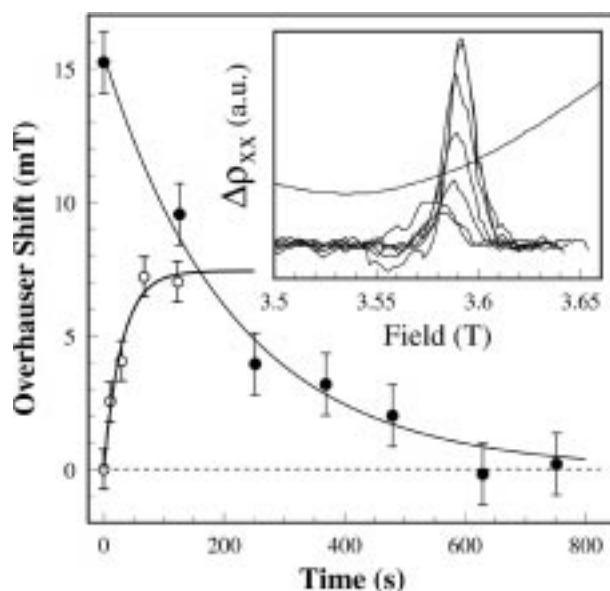


**Figure 1.** ESR spectra, after non-resonant background subtraction, acquired following a 154s optical exposure at 784nm and  $I=180\text{mW/square cm}$ . (b) ESR spectra following microwave DNP, as described in the text. In each case the nuclear relaxation was followed by repeated field up-sweeps. Open circles: nuclear field due to exposure to unpolarized light, yielding a polarization time constant of 30.4s. Filled circles and crosses: relaxation decays of the nuclear field following optical and microwave DNP, yielding 214s and 280 time constants, respectively. The microwave DNP induced Overhauser shift has been scaled down by a factor of 10.

coupling constant of  $3.7\text{ T} \pm 0.5\text{ T}$ . The significance of enhanced nuclear hyperfine fields in the quantum Hall effect is discussed.

#### Reference:

- <sup>1</sup> Dobers, M., *et al.*, Phys. Rev. Lett., **72**, 1650 (1988).



## Optical Spectroscopy of Cyclotron Resonance, Electron-Phonon Interaction and Magnetic-Field-Induced Localization in GaAs/AlGaAs Quantum Well Structures

Wang, Y.J., NHMFL

McCombe, B.D., State Univ. of New York at Buffalo,  
Physics

Schaff, W., Cornell Univ., School of Engineering

We have studied magneto-photoluminescence (PL) in two modulation-doped GaAs/AlGaAs MQW samples (24 nm/48 nm,  $3 \times 10^{11}$  and  $6 \times 10^{11} \text{cm}^{-2}$ ) in fields up to 30 T. Both samples show similar behavior scaled by filling factor,  $\nu$ . For the lower density sample below  $\nu < 4$  the PL spectra show linear-in-field Landau-level (LL) to LL transitions. For  $4 > \nu > 2$  the slopes of the LL transitions are smaller, and exhibit an upward cusp at  $\nu = 2$ . For  $\nu < 2$  the dominant feature between  $\nu = 2$  and 1 behavior is an exciton-like line. When  $\nu < 1$ , in addition to the main features, there are two transitions which appear at the *lower* energy side of the main transition. The temperature dependence study of these features at high fields shows interesting results. At 4.2 K, there are four peaks, A, B, C, and D. When the temperature is slightly increased, the original dominate transition (A) regains dominance at the expense of the low energy lines, at meantime, another line, 1, starts to appear at *high* frequency side of line A. Line 1 gains its intensity with the temperature at the expense of line A, and becomes the most dominant above 40 K, while lines B, C and D lose their intensities gradually with the temperature, and disappears above 40 K. Line A is always observable up to 70 K. Our experimental results can be understood based upon the so-called magnetic-field-induced spatial localization of the 2DEG. We believe that line B is from the recombination of an electron-hole pair bound (thus an  $X^-$ ) in the lateral vicinity of an electron confined by the long-

range potential fluctuation, while line A is from the recombination of an electron-hole pair with the electron being confined in a valley of the long-range potential fluctuation. Line 1 can thus be considered as the recombination of electron-hole pair with the electron being free.

A systematic study of electron cyclotron resonance (CR) in two sets of GaAs/AlGaAs modulation-doped quantum-well samples (12 nm/24 nm) has been carried out in magnetic fields up to 30 T. Polaron CR is the dominant transition in the region of GaAs optical phonons for the set of lightly doped samples, and the results are in good agreement with calculations that include the interaction with interface optical phonons. The results from the heavily doped set are markedly different. At low magnetic fields (below the GaAs reststrahlen region), all three samples exhibit almost identical CR which shows little effect of the polaron interaction due to screening and Pauli-principle effects. Above the GaAs LO-phonon region ( $B > \sim 23$  T), the three samples behave very differently. For the most lightly doped sample ( $3 \times 10^{11} \text{cm}^{-2}$ ) only one transition minimum is observed, which can be explained as screened polaron CR. A sample of intermediate density ( $6 \times 10^{11} \text{cm}^{-2}$ ) shows two lines above 23 T; the higher frequency branch is indistinguishable from the positions of the single line of the low density sample. For the most heavily doped sample ( $1.2 \times 10^{12} \text{cm}^{-2}$ ) there is no evidence of a high frequency resonance, and the strong, single line observed is indistinguishable from the lower branch observed from sample with intermediate doping density. We suggest that the low frequency branch in our experiment is a magnetoplasmon resonance red-shifted by disorder, and the upper branch is single-particle-like screened polaron CR.

# Pressure Effects on Magnetic Field Induced Type I-Type II Transition in CdTe/(Cd, Mn)Te Single Quantum Wells

Yokoi, H., NHMFL/LANL, Nat. Inst. of Materials and Chemical Research, Japan

Tozer, S.W., NHMFL

Kim, Y., NHMFL/LANL

Takeyama, S., Himeji Inst. of Tech.-Japan, Faculty of Science

Karczewski, G., Polish Academy of Sciences, Physics

Wojtowicz, T., Polish Academy of Sciences, Physics

Kossut, J., Polish Academy of Sciences, Physics

The heavy-hole band with  $m_j = -3/2$  of the  $\text{Cd}_{1-x}\text{Mn}_x\text{Te}$  barrier layers exhibits a large Zeeman shift due to  $sp-d$  hybridization by the application of magnetic fields. This Zeeman shift could be large enough to exceed a band offset with a sufficiently large field. In the present work, we study the effects of pressure on the magnetic field induced type I-type II transition in  $\text{CdTe}/\text{Cd}_{1-x}\text{Mn}_x\text{Te}$  ( $x=0.24$ ) single quantum wells (SQW). In the experiments, a newly commissioned 60 T long-pulsed magnet was employed. High hydrostatic pressures, up to 2.45 GPa, were obtained using a diamond anvil cell with a plastic body that is not heated up by the application of pulsed fields. Photoluminescence (PL) spectra of a heavy-hole ( $m_j = -3/2$ ) exciton were measured at 4 K, at a rate of one frame per 2 msec, that enables us to obtain PL spectra semi-continuously as a function of the magnetic field. The observed Zeeman shifts (ZS) of the PL peak for both the 48 nm thick barrier, and the 1.9 nm thick quantum well, at various pressures as shown in Figure 1. The ZS for the barrier is Brillouin function-like below about 15 T, and linear above there up to the highest fields. In contrast to this, an additional red shift is observed clearly in the ZS for the quantum well, as indicated by the arrows. The onset field of the additional red shift increases with increasing pressure. Compared with calculations for a finite quantum well, this additional red shift is attributed to a superlinear

shift of the lowest subband with respect to the concurrently decreasing barrier height. Therefore, we can regard the additional red shift as a phenomenon preceding the type I-type II transition. The increase of the onset, with increasing pressure, would bring the first experimental suggestion for pressure effects on the type I-type II transition. We estimate the critical fields for this transition to be 61 T, 68 T, and 74 T for the ambient pressure, and 1.11 GPa and 1.46 GPa, respectively, judging from the ZS, for the barrier. Further investigation with higher magnetic fields is required in order to clarify the pressure dependence of the transition field.

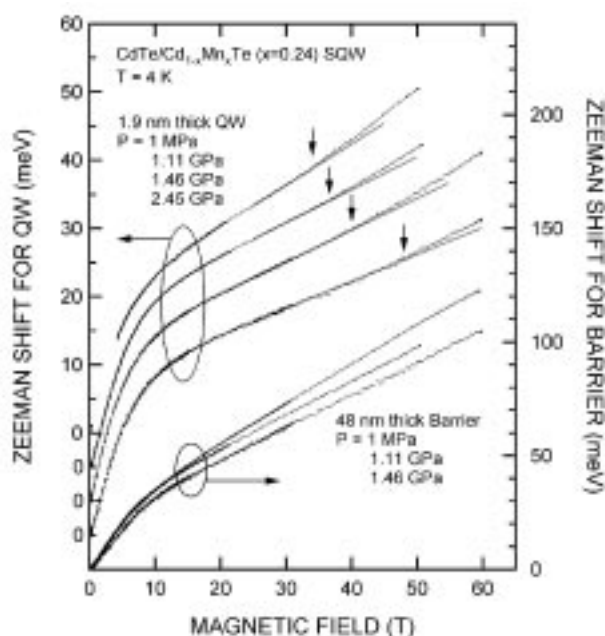


**Figure 1.** Zeeman shifts of a heavy-hole ( $m_j = -3/2$ ) exciton PL peak for a 1.9 nm thick quantum well (left axis), and a barrier (right axis), in  $\text{CdTe}/\text{Cd}_{1-x}\text{Mn}_x\text{Te}$  ( $x=0.24$ ) single quantum wells (SQWs). The onsets of additional red shifts, observed for the quantum well, are indicated by the arrows.

# High Magnetic Field Corrections to Resistance Thermometers at Low Temperatures

NHMFL

Zhang, B., NHMFL/Boston College, Physics

Brooks, J.S., NHMFL/FSU, Physics

Perenboom, J.A.A., Univ. of Nijmegen-The Netherlands

Han, S.-Y., NHMFL/FSU, Physics

Qualls, J.S., FSU, Physics

Resistance sensors such as RuO<sub>2</sub> and Cernox<sup>1,2</sup> have been widely used as thermometers at low temperatures. However, with the expanding range of magnetic fields, and temperatures at high magnetic facilities, temperature errors due to magnetoresistance effects may occur in certain limits, if based on the zero field calibration. There are several alternatives to adjusting for these high field magnetoresistance effects.<sup>3</sup> Here, we show how, with a simple calibration procedure, one can obtain reliable values of the temperature from resistive sensors, based only on the value of the resistance and magnetic field for any specific data point.

It is necessary to first establish a calibration curve of resistance vs. temperature at zero field. We have found that a polynomial expansion of the log of the temperature in terms of the log of the resistance provides an excellent fit to the resistivity.<sup>4</sup> The second crucial step is to obtain a set of isothermal curves of the resistance of the sensor vs. magnetic field.<sup>4</sup> We have used polynomial fits in our application, with terms as are needed to describe the data.

The key feature of our method is to compute, based on a single value of the resistance at a field, the corresponding value of resistance at zero field. By this the temperature can be computed from zero field calibration. We consider the relation:

$$R_i(B) = \sum_n b_{ni} (R_0(T_i)) \times B^n \quad (1)$$

$$\text{and} \quad b_n(R_0(T_i)) = \sum_m (d_{nm} \times R_0(T_i)^m) \quad (2)$$

Temperature is implicit in the zero field resistance according to  $R_0(T_i)$ . We may, therefore, expand each coefficient  $b_n(R_0(T_i))$  in terms of a polynomial in  $R_0(T)$  to obtain the final set of coefficients ( $d_{nm}$ ). The results ( $d_{nm}$ ) are illustrated in Figure 1. Once all coefficients are determined, Equation 1 can be expressed as more general function of B and T:

$$R(B) = \sum_{n,n} d_{nm} \times R_0(T)^m \times B^n \quad (3)$$

Equation 3 can be solved for  $R_0(T)$  by standard root search methods, given  $R(B)$  and B at any data point.<sup>4</sup> With the value of  $R_0(T)$ , which corresponds to  $R(B)$ , determined, the temperature may be obtained from the original calibration relation.

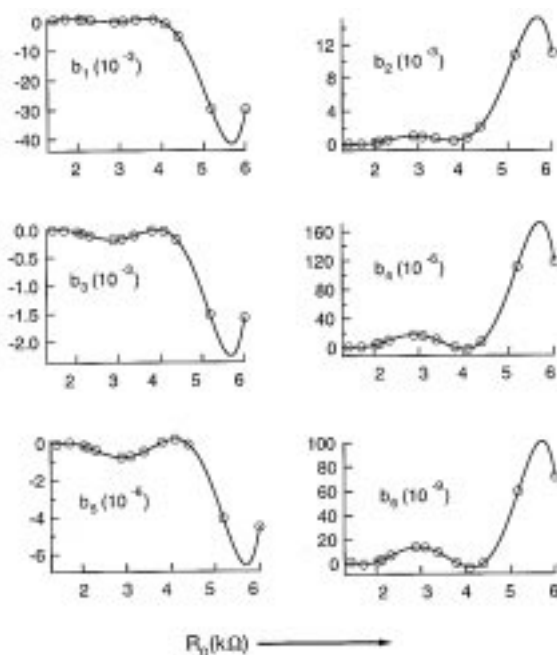


**Figure 1.** The dependence of the coefficients  $b_n$  on  $R_0$ . Solid lines 6<sup>th</sup> order polynomial fits in  $R_0$  to determine the coefficients  $d_{nm}$ . The units of the coefficients are  $\Omega T^{-1}$ .

As an example, we treat an experiment on a 200 layer GaAs/AlGaAs structure.<sup>4</sup> The calibrated 1000 $\Omega$  RuO<sub>2</sub> sensor in the mixing chamber of an Oxford Instruments top-loading dilution refrigerator was used to monitor the temperature during field sweeps to determine the

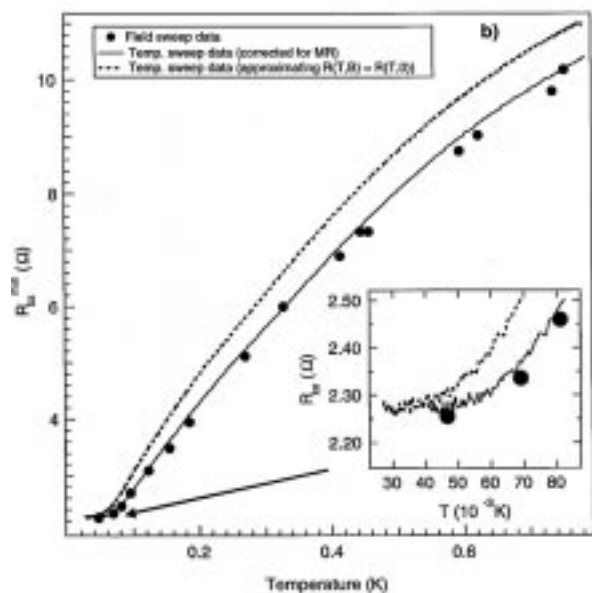


**Figure 2.** Temperature dependence of  $R_{xx}$ . Symbols - data from isothermal field sweeps; solid line - data from a temperature sweep at constant field (8.6 T) with temperature corrected for magnetoresistance; dashed line - same data without correction. Inset: expanded view of low temperature region.

magnetoresistance ( $R_{xx}$ ) in a standard transport measurement. For each temperature at which a field sweep was made. Of interest in this particular experiment was the temperature dependence of the  $R_{xx}^{\min}$  at magnetic field 8.7 T.

This may be accomplished in two ways—either by systematic isothermal field sweeps to pick off the  $R_{xx}^{\min}$ , or more conveniently, by fixing the field at 8.7 T, and changing the temperature. In the latter case, however, there will be considerable error in temperature if the magnetoresistance is not accounted for. In Figure 2, a comparison of the two ways of data acquisition is shown. The discrete points are the field sweep data where  $R_{xx}^{\min}$  is picked off of each isothermal magnetoresistance curve, and the continuous data are  $R_{xx}^{\min}$  vs. the temperature, as determined from our method that accounts for the magnetoresistance of the thermometer. Also shown is the same data, without the magnetoresistance correction.

This work is supported by NHMFL/IHRP-500/501.

#### References:

- 1 Koppetski, N., *Cryogenics*, **23**, 559(1983).
- 2 Doi, H., *et al.*, Proc. LT-17 Karlsruhe, FRG North Holland, Amsterdam, The Netherlands, 405 (1984).
- 3 Li, Q., *et al.*, *Cryogenics*, **26**, 405 (1986).
- 4 Zhang, B., *et al.*, *Scientific Instruments* (accepted).

## Quantum Hall Effect in 200 Layer GaAs/AlGaAs Multiple Quantum Well Structures

NHMFL

Zhang, B., NHMFL/Boston College, Physics  
 Brooks, J.S., NHMFL/FSU, Physics  
 Wang, Z., Boston College, Physics  
 Simmons, J., Sandia National Laboratory (SNL)  
 Reno, J., SNL  
 Lumpkin, N., Univ. of New South Wales, Australia  
 O'Brien, J., Univ. of New South Wales, Australia  
 Clark, R., Univ. of New South Wales, Australia

Periodic layers of 2 dimensional electron gas (2DEG) quantum well (QW) structures allow control over the inter-layer coupling, and, therefore, the dimensionality from 2D to 3D. If the interlayer tunneling rate ( $t$ ) is small compared to the 2D quantum Hall (QH) gap  $E_g = \hbar\omega_c$ , the bulk 3D QHE will show up. There are currently two experimental realizations of such system: 2DEG multilayers;<sup>1,2</sup> and the Bechgaard salts,  $(\text{TMTSF})_2\text{X}$ , where  $\text{X}=\text{PF}_6$ ,  $\text{ClO}_4$ , or  $\text{ReO}_4$ , that exhibit simultaneous field-induced spin density waves and QHE.<sup>3,4</sup> More surprisingly, a novel class of anisotropic 2D electron phases that exhibit metallic conductivities much smaller than  $e^2/h$  can envelope the surface of the bulk QH samples,<sup>1,5,6</sup> i.e., the chiral edge states.

The samples used in the present study were prepared by MBE. The structure contains 200 periods of 19 nm GaAs quantum wells separated by Si  $\delta$ -center-doped ( $n_d = 4.0 \times 10^{11} \text{cm}^{-2}$ )

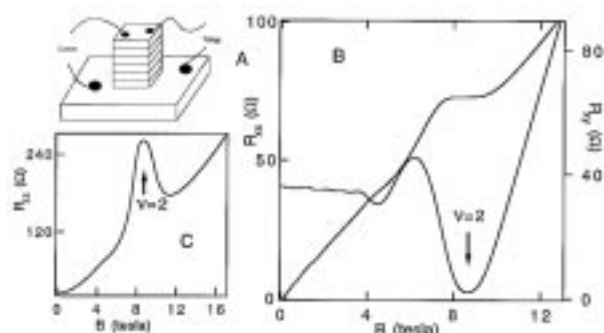


**Figure 1.** (A) Sample configuration for  $R_{zz}$  measurements. (B) Magnetoresistance  $R_{xx}$  and Hall resistance  $R_{xy}$  as a function of magnetic field at 30 mK. (C) Magnetic field dependence of  $R_{zz}$  at 30 mK.

$\text{Al}_{0.1}\text{Ga}_{0.9}\text{As}$  barriers of thickness 4 nm. To prevent layer depletion and offset the surface pinning potential, a cap layer and a sequence of  $\text{Al}_{0.1}\text{Ga}_{0.9}\text{As}$  doped layers were grown.<sup>6</sup> A Hall bar configuration was used in measuring in-plane magnetoresistance ( $R_{xx}$  and  $R_{xy}$ ). To study the chiral edge state through vertical transport,  $R_{zz}$ , mesa configurations were prepared for the same samples as shown in Figure 1a. Figure 1b shows  $R_{xx}$  and  $R_{xy}$  versus magnetic field at 30 mK. At 8.7 T, concomitant with  $R_{xx}$  minima, there is a well developed plateau, which saturates at  $64.45 \pm 0.010 \Omega$ . This value corresponds to a quantization of  $R_{xy} = (1/200)(\hbar/2e^2)$ , and demonstrates a spin-unpolarized integer QHE at the filling factor  $\nu = 2$ .  $R_{xx}$  in low field exhibits SdH oscillation. Figure 1c presents the field dependence of  $R_{zz}$  at 30 mK. Around 8.7 T, there is a peak corresponding to the minimum of  $R_{xx}$  at  $\nu = 2$ . Using  $R_{xx}^{\min}$  and  $R_{zz}^{\max}$  as the value of  $R_{xx}$ , and  $R_{zz}$  at  $\nu = 2$ , respectively, we studied their temperature and in-plane field ( $B_{\perp}$ ) dependence as shown in Figure 2. A and B panels are  $R_{xx}^{\min}$  and  $1/R_{zz}^{\max}$  versus temperature inverse. At low temperature ( $T < 270$  mK) both fit the Coulomb gap form (Equation 1), and at high temperature ( $2 \text{ K} > T > 270$  mK), they fit the activation form (Equation 2).

$$R = R_{res} + R_0 e^{-\sqrt{T_c/T}} \quad (1)$$

$$R = R_0 e^{-(\Delta/2KT)} \quad (2)$$

C and D panels show the in-plane field (angle) dependence of  $R_{xx}^{\min}$  and  $1/R_{zz}^{\max}$ . It is interesting to find that both exhibit optimal value of  $B_{\perp}$  (angle).  $R_{xx}^{\min}$  and  $1/R_{zz}^{\max}$  seem to present the same behavior. Work is presently under the way to explore these unusual results.

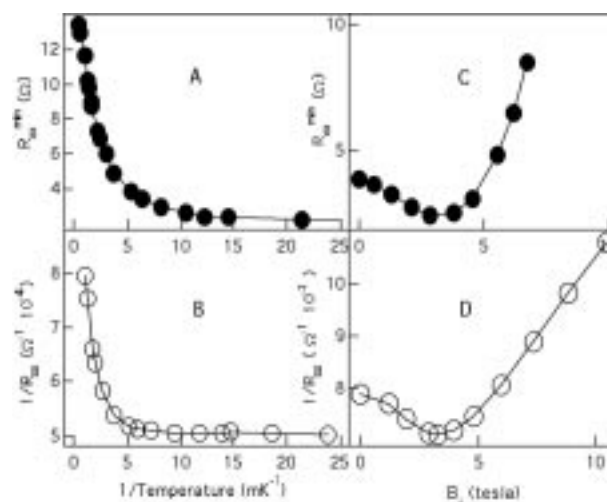


**Figure 2.** (A) Temperature dependence of  $R_{xx}^{\min}$  at zero titled angle. (B) Temperature dependence of  $1/R_{zz}^{\max}$  at zero titled angle. (C) In-plane field (angle) dependence of  $R_{xx}^{\min}$ . (D) In-plane field (angle) dependence of  $1/R_{zz}^{\max}$ .

This work is supported by NHMFL/IHRP-500/5011.

#### References:

- 1 Druist, D.P., *et al.*, Phys. Rev. Lett., **80**, 365 (1998).
- 2 Stormer, H.L., *et al.*, Phys. Rev. Lett., **56**, 85 (1986).
- 3 Balicas, L., *et al.*, Phys. Rev. Lett., **75**, 2000 (1995).
- 4 Poilblanc, D., *et al.*, Phys. Rev. Lett., **58**, 270 (1995).
- 5 Balents, L., *et al.*, Phys. Rev. Lett., **76**, 2783 (1996).
- 6 Zhang, B., *et al.*, Physica B, (accepted).